Application of Yeast to Understanding the Mode of Action of the Antimalarial Drug Artesunate

Jonathan M. Wilson, BSc.

Thesis submitted to the University Of Nottingham for the degree of Master of Research

December 2014

Abstract

The aim of this project was to use the budding yeast model, *Saccharomyces cerevisiae,* in order to investigate the mode of action of the antimalarial drug artesunate. Using a range of techniques and resources available for *S. cerevisiae*, the research has identified two potential genes of interest, *CDC73* and *ADH1*. The absence of either one of the genes causes increased sensitivity to artesunate in *S. cerevisiae* grown in the rich broth medium, YEPD. Such sensitivity of both deletion strains was only apparent on fermentable medium. Overexpressing both *CDC73* and *ADH1* in wild type backgrounds had no effect on the sensitivity of yeast to artesunate, suggesting that neither are direct targets of the drug. The increased sensitivity of the *adh1Δ* mutant relative to the wild type was dependent on the presence of oxygen whereas that of *cdc73Δ* cells appeared not to be. It was not possible within the timeframe of the project to discern why *cdc73Δ* yeast cells experience heightened sensitivity to artesunate, but it was established that they are able to produce ethanol and that they show higher intracellular superoxide than wild type cells. The cause of the *adh1Δ* mutant's increased sensitivity to artesunate was hypothesised to be a shift in metabolism towards aerobic respiration, resulting in activation of the drug. The dependence of *adh1Δ* cells' increased sensitivity to artesunate on the presence of oxygen is consistent with existing models of artemisinin damage to yeast cells that are characterised by reactive oxygen species production. Because the *cdc73Δ* mutant potentially remains hypersensitive to artesunate

in anaerobic conditions it suggests that artesunate damage may not be mediated via reactive oxygen species, which suggests that the two genes most likely confer artesunate resistance in wild type cells by different mechanisms. This could be consistent with the possibility of at least two mechanisms by which artesunate causes growth inhibition in yeast.

Acknowledgements

I would like to thank my supervisor Dr Simon Avery for giving me the opportunity to work in his lab, and for all of his help, support, and patience throughout my project.

I would also like to thank Sarah Tindall, Cindy Vallieres, and Lee Shunburne for all of their assistance and advice during my time in the lab.

Many thanks to Chris Powell and Sarah Nicholls from the School of Biosciences for their help, advice, and use of equipment for the fermentations performed on Sutton Bonington campus.

I wish to thank my family, Mum, Dad, Sarah and David for their support throughout the past year.

Thank you to my flatmates, James Brown, Tim Dixon, Brad Heath, Dan Lilley, and Rich McLernon, for a fantastic year in Flat 2.

Finally I extend special thanks to my grandparents, Dr J and Mrs M Wilson, without whom this would not have been possible. Thank you for your unwavering support.

Table of Contents

1. Introduction 8

1.1 Malaria 8

1.2 Treatment of malaria 9

1.3 Artemisinins as antimalarial drugs 11

1.4 *Saccharomyces cerevisiae* as a model organism 15

1.6 Antimalarial mode of action research in the *S. cerevisiae* model 16

1.7 Project aims 19

2. Materials and Methods 20

2.1 Strains, media, and growth conditions 20

2.2 Stock solutions 22

2.3 PCR and primers 23

2.4 Yeast growth curves 25

2.5 Yeast genomic DNA extraction 25

2.6 Plasmid minipreps 26

2.7 Plasmid constructions 27

2.8 Yeast Transformations 30

2.9 Dihydroethidium superoxide assay 30

2.10 Generation of petite mutants 31

2.11 Fermentations 32

2.12 Spotting assays 33

2.13 Assay for *RAD54-GFP* activation 34

3. Results 36

3.1 Artesunate inhibits growth of yeast on both fermentable and non-fermentable carbon sources 36

3.2 The yeast deletion mutant *cdc73Δ* shows increased sensitivity to artesunate on YEPD medium 37

3.3 Overexpression of *CDC73* in a WT background does not affect artesunate sensitivity 40

3.4 The deletion mutants *leo1Δ*, *rtf1Δ*, *pdc1Δ*, *pdc5Δ* and *pdc6Δ* do not show increased sensitivity to artesunate on YEPD medium 43

3.5 The *cdc73Δ* mutant shows higher intracellular reactive oxygen species than WT when grown on YEPD 47

3.6 Artesunate may not be genotoxic 50

3.7 Comparison of WT and *cdc73Δ* yeast growth pre- and post-diauxic shift 52

3.8 Petite mutants of WT and *cdc73Δ* cells show increased sensitivity to artesunate on YEPD medium 53

3.9 The *cdc73Δ* mutant is capable of ethanol production 57

3.10 Repeat of tests for diauxie during WT and *cdc73Δ* yeast growth 60

3.11 Hyper-sensitivity of the *cdc73Δ* mutant to artesunate may not be dependent on the presence of oxygen 61

3.12 The yeast deletion mutant *adh1Δ* shows increased sensitivity to artesunate on YEPD medium 62

3.13 Extracellular ethanol concentration does not affect sensitivity of *adh1Δ* cells to artesunate on YEPD medium 63

3.14 Overexpression of *ADH1* in WT and *cdc73Δ* backgrounds does not improve artesunate resistance 64

3.15 Increased sensitivity *of adh1Δ* cells to artesunate is dependent on the presence of oxygen 68

3.16 Increased sensitivity to artesunate in *adh1Δ* cells is not a consequence of a change in the activity of the glycerol production pathway 69

4. Discussion 73

4.1 Cdc73p and the Paf1p complex 73

4.2 Superoxide levels in WT and *cdc73Δ* strains of yeast 74

4.3 Ethanol production by *cdc73Δ* cells 75

4.4 Diauxie in WT and *cdc73Δ* yeast cultures 76

4.5 The role of oxygen in artesunate hypersensitivity of the *cdc73Δ* mutant 77

4.6 Inconsistent behaviour of the *cdc73Δ* mutant 78

4.7 Hyper sensitivity of *cdc73Δ* cells to artesunate is unrelated to a lack of Adh1p 79

4.8 Hypersensitivity to artesunate of the *adh1Δ* mutant 79

4.9 Genotoxicity assays 80

4.10 Conclusions 81

5. References 85

6. Appendix 96

1. Introduction

1.1 Malaria

Malaria is an infectious disease caused by protozoans of the genus *Plasmodium*. Human infection is usually from one of four species, *P. falciparum*, *P. vivax*, *P. malariae*, or *P. ovale*. *P. falciparum* causes the most severe form of malaria (Ferri 2009). The life cycle of *Plasmodium* takes place between two hosts, mosquitos and mammals. *Plasmodium* is transmitted via bites from female *Anopheles* mosquitos, which introduce the parasite into the host's blood. Once in the bloodstream, sporozoites of the parasite migrate to hepatocytes in the liver where they undergo asexual reproduction to produce merozoites. At the end of the liver stage, merozoites are released back into the bloodstream where they infect red blood cells (erythrocytes). During the erythrocyte stage, merozoites either continue reproducing asexually or will develop into gametocytes. When a mosquito then bites the infected mammalian host to feed, it also ingests gametocytes. In the mosquito digestive system the gametocytes mature into gametes which are able to fertilise each other to form an ookinete. The ookinetes will develop into new sporozoites which will migrate to the mosquito salivary glands and the cycle can continue (Cox 2010).

Symptoms of malaria manifest themselves during the mammalian blood stage of the *Plasmodium* life cycle. All forms of malaria show early symptoms resembling flu, but in later stages of the disease, severe malaria can affect the

cerebral, respiratory, and renal systems, as well as causing severe anaemia (Bartoloni and Zammarchi 2012).

The total number of deaths caused by malaria in 2012 is estimated to be 627,000 people (World Health Organisation 2014). Although primarily confined to tropical regions, there is increasing concern that higher temperatures due to climate change may increase the distribution of *Anopheles* and with it spread malaria to new regions (Chaves and Koenraadt 2010).

1.2 Treatment of malaria

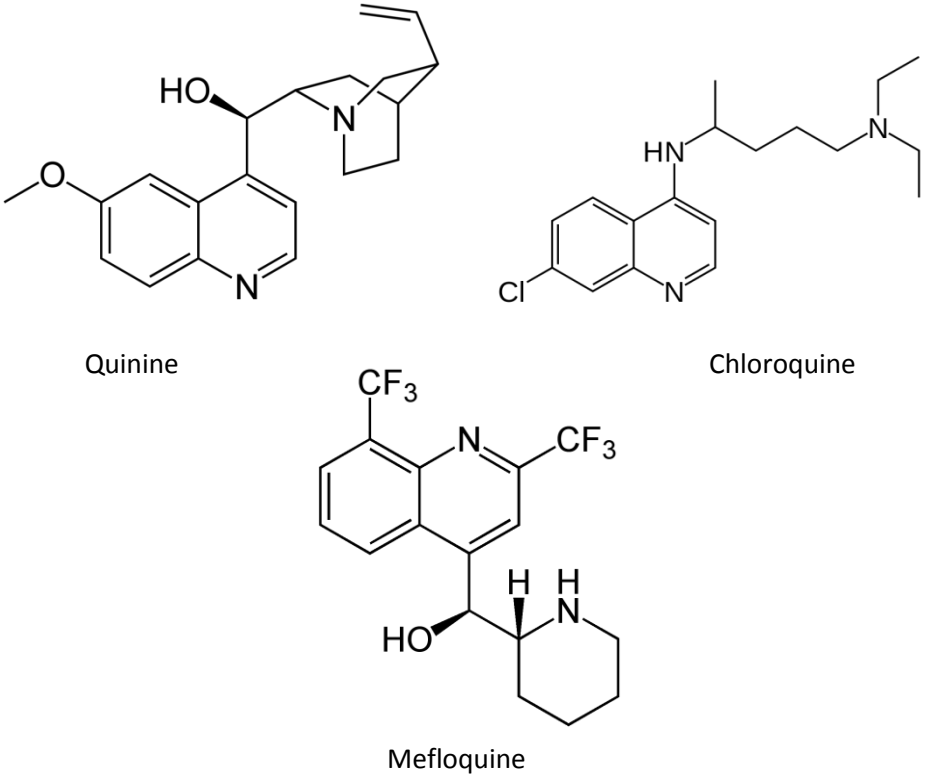
One of the first effective treatments for malaria patients was the drug quinine (Figure 1). Quinine is an alkaloid that occurs naturally in the bark of the cinchona tree and has been used to treat malaria at least as far back as the early 1600s (Achan et al. 2011). Although quinine still remains an effective treatment of malaria in some areas, reports of quinine resistant malaria from the Thai-Cambodian border have been noted since the 1960s (Wongsrichanalai et al. 2002). Quinine treatment has long been associated with adverse drug reactions (ADRs), ranging from sweating and nausea to severe vomiting and diarrhoea (Bateman 1986). The mechanism of action of quinine against *Plasmodium* is not fully elucidated, but it is thought to be similar to that of the related antimalarial drug, chloroquine (Figure 1).

Chloroquine was discovered by German scientist Hans Andersag in 1934, but it wasn't until the end of the Second World War that it became

accepted as a viable alternative to quinine (Centers for Disease Control and Prevention 2012). Chloroquine kills malaria parasites by inhibiting the detoxification of haem. Once *Plasmodium* merozoites infect red blood cells, they digest haemoglobin as a source of nutrients; Digestion also releases haem compounds. Normally the parasite detoxifies the haem by bio-crystallising it to haemozoin. Chloroquine however inhibits crystallisation which leads to the accumulation of haem, killing the cell (Hempelmann 2007). Resistance to chloroquine has been noted in *Plasmodium*; the exact mechanism is not completely understood, however it is known to be associated with the parasite protein PfCRT. This protein is involved in removing chloroquine from the parasite, which prevents the drug reaching concentrations that can inhibit haem detoxification (Chinappi et al. 2010). Unfortunately, strains of chloroquine-resistant *Plasmodium* are now widespread (World Health Organisation 2014). Some estimates are as high as 80% of all *Plasmodium* parasites (Singh and Singh 2014).

Another quinine-related drug is mefloquine (Figure 1). As well as being used to treat people already suffering from malaria, mefloquine can be taken prior to entering a malaria endemic area to prevent infection. It is not recommended for treatment of severe cases of malaria. Although serious neurological and psychiatric problems have been associated with mefloquine use, they have been shown to be rare and it is still considered a first line chemoprophylactic. Users should be informed of potential side effects and medical histories should be considered prior to prescription (Schlagenhauf et

al. 2010). Like quinine, its mode of action against *Plasmodium* is thought to be similar to that of chloroquine (Singh and Singh 2014).



Quinine Chloroquine

Mefloquine

Figure 1. Molecular structures of quinine, chloroquine and mefloquine. Images courtesy of Wikimedia Commons.

1.3 Artemisinins as antimalarial drugs

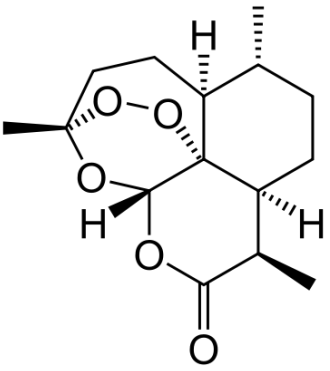
In the 1960s and 70s the Chinese government conducted a screen of over 2,000 traditional Chinese medicines for anti-malarial activity, named the 523 Project (Tu 2011). In 1971 researchers isolated the drug artemisinin (Figure 2) from the plant *Artemisia annua* 'Sweet wormwood' (Hommel 2008). The earliest known reference to medicinal use of *A. annua* was in a prescription handbook from the Chinese Jin Dynasty (265-420) recommending it as a treatment of intermittent fever (Hsu 2006). Artemisinin

and its derivatives are highly effective treatments of malaria. They are primarily used in conjunction with other anti-malarial drugs (usually quinine derivatives) in order to minimise chances of resistance developing. The World Health Organisation currently recommends artemisinin based combination therapies (ACTs) as the best available treatment for malaria. Although potent, artemisinin quickly degrades *in vitro*, and so research lead to the development of more stable derivatives. Artesunate (Figure 2) is a semi-synthetic derivative of artemisinin that has the distinct advantage over its precursor of being water soluble, and as such can be administered via injection (Hommel 2008). Artemether (Figure 2) is another derivative of artemisinin, commonly administered in combination with a synthetic antimalarial drug, lumefantrine (Figure 3). This combination is commonly referred to as co-artemether. In one study, this combination was shown to produce a 96% cure rate of children in Uganda (Achan et al. 2009). Dihydroartemisinin (Figure 2) is the active metabolite of all artemisinins, but can also be taken directly, usually in combination with piperaquine (Figure 3) (Faurant 2011). A common feature of the molecular structure of artemisinin and its derivatives is the presence of an endoperoxide bridge. It is thought that cleavage of the endoperoxide group is fundamental to the antimalarial activity of this class of drug (Meshnick et al. 1996).

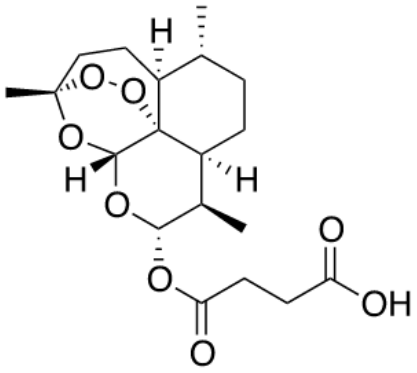
Research into the action of artemisinins in *Plasmodium berghei* cells has revealed that the drug is distributed to the mitochondria within the parasite. Artemisinins will impair the function of isolated *Plasmodium* mitochondria,

while showing increased reactive oxygen species (ROS) production and depolarisation of the parasite mitochondrial membrane (Antoine et al. 2014). The evidence also suggests that the drug may target the first stage of the electron transport chain. Suppression of reduced nicotinamide dinucleotide (NADH) dehydrogenase (the *Plasmodium* equivalent of the mitochondrial complex I of higher eukaryotes) activity reduces artemisinin sensitivity of the parasite (Wang et al. 2010).

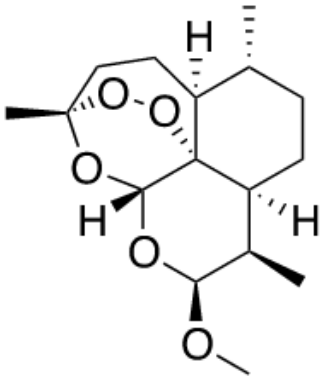
Despite the fact that artemisinins are widely used to treat malaria, their principal mode(s) of action against the parasite is still not completely understood. Elucidating this information has become increasingly important in recent years, as reports of artemisinin resistance surface in Cambodia, specifically in regions close to the Thailand border (Miotto et al. 2013), the same region where frequent reports of quinine resistance first emerged. The hope is that once the mode of action of the drugs is characterised, it may be possible to discern more clearly how *Plasmodium* has developed resistance and, therefore, how this can be effectively combated. Because the mechanism of action is still poorly characterised and *Plasmodium* spp. are not especially amenable to studies in the laboratory, some researchers have turned to using alternative models to study artemisinins, including the yeast *Saccharomyces cerevisiae*.



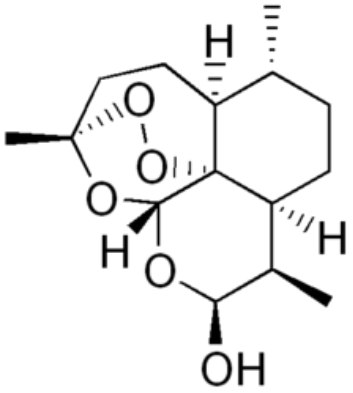
Artemisinin



Artesunate

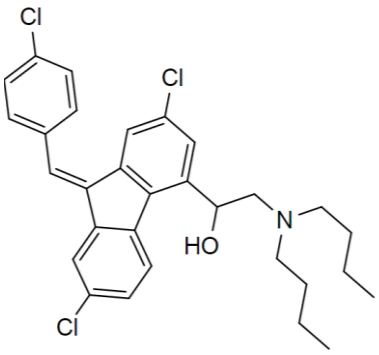


Artemether

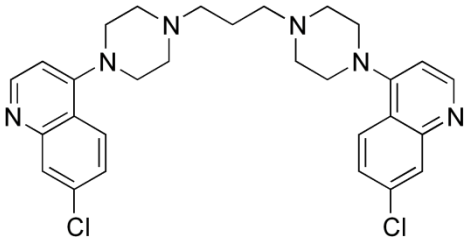


Dihydroartemisinin

Figure 2. Molecular structures of artemisinin, artesunate, artemether, and dihydroartemisinin. Images courtesy of Wikimedia Commons.



Lumefantrine



Piperaquine

Figure 3. Molecular structures of lumefantrine and piperaquine. Images courtesy of Wikimedia Commons.

1.4 *Saccharomyces cerevisiae* as a model organism

Saccharomyces cerevisiae (*S. cerevisiae*) is a species of budding yeast that has been historically exploited by humans for the purposes of brewing and baking. It was the first eukaryotic organism to have its genome fully sequenced, and has also become one of the most extensively studied model organisms. Early research showed that ~31% of yeast genes have homologues in mammals, but this is thought to be an underestimate (Botstein et al. 1997). It is also generally accepted to share ~900 orthologous proteins with *P. falciparum* (Wuchty et al. 2006). *S. cerevisiae* is often used to study human disease at the cellular level due to the conservation of fundamental processes between these eukaryotes (Bolotin-Fukuhara et al. 2010). Along with its physiological similarities with higher eukaryotes, yeast has many advantageous properties that make it an ideal model organism for research. These include uncomplicated and inexpensive culture; short generation time, cells can divide in less than two hours; it is relatively easy to manipulate genetically, gene knockouts and insertions are achieved efficiently via homologous recombination and cells can also be transformed with plasmids; it can also exist in both haploid and diploid forms.

Because of the extent to which yeast has been studied, there is a wealth of existing resources available to researchers, including the Yeast Deletion Strain collection. This is a genome-wide collection of *S. cerevisiae* strains each containing a deletion of one specific gene, and in its place a kanamycin resistance cassette (KanMX) (Winzeler et al. 1999). The combined

libraries contain over 20,000 strains, of which approximately 4,800 are homozygous diploid strains from the BY4743 background. The library became the basis on which synthetic genetic arrays were developed; high throughput crossing of the haploid strains in the library lead to production of double mutants that can be screened for changes in fitness, or 'synthetic lethality'. This technique has proved a powerful tool for gaining knowledge of genetic interactions (Scherens and Goffeau 2004). Single deletion mutants have been used to research mode of action of drugs, as well as to assay new compounds for known drug-like activity (Smith et al. 2010).

1.6 Antimalarial mode of action research in the *S. cerevisiae* model

The experimental advantages of *S. cerevisiae* have been exploited as a model to research the effects of antimalarial compounds. Research in the Avery laboratory into the toxicity of quinine using mutants from the Yeast Deletion Strain collection revealed that quinine inhibits the uptake of tryptophan by yeast cells, eventually leading to tryptophan starvation. The results indicated that the mechanism by which this occurs is competitive inhibition (Khozoie et al. 2009). Subsequently, it was shown that malaria patients with low tryptophan levels appeared predisposed to adverse reactions to quinine (Islahudin et al. 2012). Building further on this research, quinine was found to disrupt synthesis and action of serotonin, a neurotransmitter that tryptophan is a precursor of (Islahudin et al. 2014). Research into chloroquine using yeast deletion mutants has revealed that the

BLK1 and *SLT2* genes are required for yeast resistance to the drug. These genes are involved in maintaining cell wall integrity, and their disruption lead to increased chloroquine accumulation within the yeast cells (Islahudin et al. 2013).

Previous research on artemisinins in *S. cerevisiae* has revealed that like *Plasmodium berghei*, a primary target of the drug is the mitochondria. A 2005 paper by Li et al. proposed that artesunate becomes activated by electron transport chain activity, which causes the drug to generate free radicals which in turn damage the cell by depolarising the mitochondrial membrane. Li et al. (2005) also found that deletion of either *NDE1* or *NDI1* (The genes encoding two NADH dehydrogenases of the yeast electron transport chain) would confer a level of artesunate resistance to the cells, and that overexpressing them will increase the yeast's sensitivity to the drug. These findings, along with other research that shows that disruption of the other elements of the electron transport chain does not affect yeast metabolism of artemisinin (Wang and Zhou 2010) imply that NADH dehydrogenase activity plays an important role in the drug's mode of action in yeast. After treatment of yeast with deoxyartemisinin (a molecule identical to artemisinin, except lacking an endoperoxide bridge) yielded no growth inhibition of yeast, it was hypothesised that electron transport chain activity cleaves the endoperoxide group, leading to ROS production (Wang et al. 2010).

Other research using yeast has shown that the mitochondria may not be the sole targets of artemisinins. Moore et al. (2011) suggested that

artemisinins may also target ATP-dependent calcium channels. Yeast grown on a fermentable carbon source lacking the two genes which encode the two calcium channels found in *S. cerevisiae* (*PMR1* and *PMC1*) showed less sensitivity to artemisinin and artesunate than the reference strain. Addition of reducing agents (that break the endoperoxide bridge of the drug) to yeast cultures resulted in the negation of sensitivity to artemisinins of WT cells grown on fermentable medium. Conversely, hyper sensitivity to the drug was observed in WT cells grown on non-fermentable medium supplemented with reducing agents. The paper hypothesised that there are at least two mechanisms by which artemisinins can damage yeast cells; one where degradation of the drug damages the mitochondria, and another that involves specific binding of the drug, potentially to calcium channels. Furthermore, the *Plasmodium* calcium channel PfATP6 has shown to be inhibited by artemisinins when expressed in a yeast model (Krishna et al. 2014). Other targets of artesunate in yeast may be involved cell cycle progression. Steinbrück et al. (2011) reported changes in artesunate sensitivity of yeast growing in fermentable medium when deleted for genes involved in regulation of mitotic spindle synthesis.

Moore et al. (2010) also addressed degradation of artemisinins by iron (II) compounds (noted in Zhang and Gerhard 2008), in this instance haem. Additions of haem to yeast cultures in fermentable medium resulted in the negation of artemisinin and artesunate sensitivity. The explanation given was that degradation of the drug by haem renders it inactive to yeast growing on

fermentable media. Conversely, addition of haem to yeast cultures grown on a non-fermentable medium resulted in hyper-sensitivity to artemisinin and artesunate. The sensitivity could be partly alleviated by addition of a free radical scavenger. This implied that degradation of the drugs releases free radicals, which damage the mitochondria.

1.7 Project aims

The aim of this project is to use the *S. cerevisiae* model in order to gain insight into how artesunate damages cells. Identifying genes involved in normal artesunate resistance is a key step in understanding the drug's mode of action. A genome wide screen of deletion mutants for changes in artesunate sensitivity was performed by the host laboratory prior to the start of the project. The project began by selecting deletion mutants from within this screen that showed potential changes in artesunate sensitivity. The deletion mutants were investigated further in order to establish why lacking specific genes resulted in a change in artesunate sensitivity.

2. Materials and Methods

2.1 Strains, media, and growth conditions

All diploid yeast strains used throughout this project were from the *S. cerevisiae* strain background BY4743 (*MATa*/*MATα his3Δ* 1/*his3Δ* 1; *leu2Δ*0 /*leu2Δ* 0; *met15Δ* 0/*MET15*; *LYS2*/*lys2Δ* 0; *ura3Δ* 0/*ura3Δ* 0). All haploid strains used throughout this project were from the BY4741 background (*MATa*; *his3Δ* 1; *leu2Δ* 0; *met15Δ* 0; *ura3Δ* 0). WT (wild type) refers to unmodified BY4743, as described above. Wild type and single-gene deletion strains were obtained previously by the host laboratory from Euroscarf (Frankfurt). In all yeast deletion strains, the target gene had been removed (from start to stop codon) by replacement with a KanMX cassette. The complete list of deletion mutants used is given in Table 1. XL1-Blue competent *E. coli* cells were used for plasmid constructions (Stratagene).

Yeast strains were stored at 4°C on YEPD+ agar (1% yeast extract, 2% peptone, 2% glucose, 2% agar w/v) plates. Geneticin® (G418) at 100µg ml^{-1} was included in the agar plates for deletion mutants. For experiments, yeast was cultured in YEPD (1% yeast extract, 2% peptone, 2% glucose w/v) or YEPG (1% yeast extract, 2% peptone, 3% glycerol, and 0.1% glucose w/v) broth, unless stated otherwise. NB: 0.1% glucose was included in YEPG cultures to help mitigate the prolonged lag phase yeast exhibit when grown with only a glycerol carbon source.

Successfully transformed yeast cells were selected for using yeast nitrogen base (YNB) (Sigma-Aldrich) agar plates (2% glucose, 2% agar w/v). Three types of selective YNB were used in this project. YNB-His (YNB + 60mg L^{-1} leucine, 20mg L^{-1} methionine, 10mg L^{-1} uracil) was used to select for successful integration of a histidine tag into the yeast genome; YNB-Leu (YNB + 20mg L^{-1} histidine, 20mg L^{-1} methionine, 10mg L^{-1} uracil) was used to select for successful transformation of yeast with plasmids based on the pRS315 vector; and YNB-Ura (YNB + 20mg L^{-1} histidine, 60mg L^{-1} leucine, 20mg L^{-1} methionine) was used to select for successful transformation of yeast with plasmids based on the pCM190 vector. Successfully transformed *Escherichia coli* (*E. coli*) were selected using lysogeny broth (LB) agar plates (1% tryptone, 0.5% yeast extract, 1% NaCl, 1.5% agar w/v) containing 100µg ml^{-1} ampicillin.

Yeast pre-cultures were prepared by transferring a single colony to growth medium in an autoclaved conical flask, filled to one fifth of the total flask volume and sealed with a foam bung. The flasks were then placed in an incubator overnight at 30°C with shaking at 200 RPM. The following morning the cultures were measured for OD_{600}, diluted as appropriate using fresh medium and allowed to recover, ideally allowing time for at least two cell divisions before initiation of an experiment (see below).

Table 1. List of all *S. cerevisiae* single gene deletion mutants used in the project. All were from the diploid background BY4743.

Mismatch repair (MMR) gene mutants	*msh1Δ*, *msh2Δ*, *msh3Δ*, *msh6Δ*, *mlh1Δ*, *mlh2Δ*, *mlh3Δ*
Telomere related gene mutants	*cdc73Δ*, *est1Δ*, *exo1Δ*, *met18Δ*, *pms1Δ*, *rad1Δ*, *rad2Δ*, *rlf2Δ*, *sba1Δ*, *stm1Δ*, *swd3Δ*, *tel1Δ*, *xrs2Δ*, *zds2Δ*
Paf1p complex gene mutants	*leo1Δ, rtf1Δ*
Pyruvate decarboxylase gene mutants	*pdc1Δ*, *pdc5Δ*, *pdc6Δ*
Other mutants	*adh1Δ*, *gpd1Δ*

2.2 Stock solutions

150mM and 75mM stock solutions of artesunate (molecular mass 384.421 g mol^{-1}) were prepared by dissolving the appropriate amounts of artesunate (0.0288g and 0.0144g respectively) in 500µl 70% v/v ethanol. Stocks of lower concentrations were made by diluting the original stocks.

10mM dihydroethidium (DHE) stock was produced by dissolving 1.5µg DHE (molecular mass 315.41 g mol^{-1}) in 500µl dimethyl sulfoxide (DMSO). Stocks of lower concentrations were produced by diluting the original stock.

1.84M paraquat stock and 10mg ml^{-1} (~2.5mM) ethidium bromide (EtBr) stock were provided by the host laboratory, both prepared using sterile deionised water (SDW).

Single stranded (SS) carrier DNA (2mg ml^{-1}) derived from salmon testes (Sigma-Aldrich) was denatured before use by incubating in a boiling water bath for five minutes, aliquoted, and then immediately chilled on ice or stored at -20°C.

2.3 PCR and primers

All polymerase chain reactions (PCR) done in this project were performed using Phusion® High-Fidelity DNA Polymerase, from New England Biolabs (NEB) optimised using DMSO rather than $MgCl_2$. The composition of the reactions was adapted from the manufacturer's description. 100µl 5X Phusion HF buffer, 10µl 10mM dNTPs, 25µl 10µM forward primer, 25µl 10µM reverse primer, 15µl DMSO, 0.5µg template DNA, 5µl Phusion DNA polymerase, SDW to 500µl. The PCR mix was thermocycled with the following settings. Initial denaturation 98°C 30s, denaturation 98°C 10s, annealing (specific temperatures (T_m) in Table 2) 30s, elongation 72°C 30s per kilobase, final extension 72°C 5min, final hold 4°C. 30 cycles of denaturation, annealing and elongation were used, which was increased to 40 cycles in cases of low yield. Primer sequences and descriptions are given in Table 2.

Table 2. Nucleotide sequences and annealing temperatures of all primers used in the project.

Primers	Sequence	T_m	Description
RAD54-GFP fusion	**F**. 5'-acgagcatcattacaatgatatcagttttgcatttcaatatatttcacatcggatccccgggttaattaa-3' **R**. 5'-atcgaattctacttttttgttttttgttttataagtacatgtatgtaagagagaattcgagctcgtttaaac-3'	58°C	Primers made to amplify a cassette comprised of a Green Fluorescent Protein (GFP) C-terminal tag and an *ADH1* terminator sequence, followed by a His marker (HIS3MX6). The cassette is flanked by two 50bp sequences homologous to sequences either side of the stop codon of the *RAD54* gene in the yeast genome. The template DNA used was the pFA6a-GFP(S65T)-His3MX6 plasmid.
RAD54 insert	**F**. 5'-agttgtcgacgatctgtcctcttaagtaga-3' **R**. 5'-ttaattaacccggggatccgatgtgaaatatattgaaatg-3'	49°C	Primers made to amplify the promoter and sequence of the *RAD54* gene minus its stop codon, flanked by sequences to produce a *Sal*I restriction site at the 5' end, and an *Xma*I restriction site at the 3' end. The template DNA used was WT yeast genomic DNA
GFP tag insert	**F**. 5'-acgagcatcattacaatgatatcagttttgcatttcaatatatttcacatcggatccccgggttaattaa-3' **R**. 5'-aactgagctcccggtagaggtgtggtcaat-3'	64°C	Primers made to amplify the GFP C-terminal tag and *ADH1* terminator sequence, flanked by sequences to produce an *Xma*I restriction site at the 5' end, and a *Sac*I restriction site at the 3' end. Note: Forward primer is identical to forward *RAD54*-GFP fusion primer. The template DNA used was the pFA6a-GFP(S65T)-His3MX6 plasmid.
CDC73 insert	**F**. 5'-ataagaatgcggccgcatggcgaactcattagacag-3' **R**. aaaactgcagtcaacggtatcctcttgaaa-3'	59°C	Primers made to amplify the complete sequence *CDC73*, flanked by sequences to produce a *Not*I restriction site at the 5' end, and a *Pst*I restriction site at the 3' end. The template DNA used was WT yeast genomic DNA
ADH1 insert	**F**. 5'-ataagaatgcggccgcatgtctatcccagaaactca-3' **R**. aaaactgcagcgcttatttagaagtgtcaa-3'	55°C	Primers made to amplify the complete sequence of *ADH1*, flanked by sequences to produce a *Not*I restriction site at the 5' end, and a *Pst*I restriction site at the 3' end. The template DNA used was WT yeast genomic DNA
GPD1 insert	**F**. 5'-ataagaatgcggccgcatgtctgctgctgctgatag-3' **R**. 5'-aaaactgcagctaatcttcatgtagatcta-3'	50°C	Primers made to amplify the complete sequence of *GPD1*, flanked by sequences to produce a *Not*I restriction site at the 5' end, and a *Pst*I restriction site at the 3' end. The template DNA used was WT yeast genomic DNA

2.4 Yeast growth curves

Yeast pre-cultures were diluted with fresh growth medium to OD_{600} ~0.1 in the morning and allowed to recover to at least 0.4. Cultures were then diluted again to D_{600} ~0.05 and aliquots transferred to 48-well plates. Varying concentrations of the substance being assayed was then added to the cultures to make a final volume of 300µl. The plate was sealed with tape to prevent evaporation. The plate was then placed into the plate reader (Powerwave XS and XS2, Biotek), set to continuous shaking at 30°C. OD_{600} was recorded every 30 min for up to 48 h.

2.5 Yeast genomic DNA extraction

Yeast genomic DNA extractions were performed using either one of two methods. The first method was adapted from Amberg et al. 2005. 1.5ml of undiluted yeast pre-culture was microcentrifuged (16,000 x g) for 2 min in a 1.5ml microcentrifuge tube and the pellet resuspended in 200µl lysis buffer (10mM Tris pH 8.0, 1mM EDTA, 100mM NaCl, 1% SDS, 2% Triton X-100). 200µl of 1:1 phenol: chloroform and a scoop (<100µl) of glass beads (425-600µM, Sigma-Aldrich) were added to the tube and vortexed for 2 minutes. The tube was then microcentrifuged (16,000 x g) for 5 min. The resulting top layer was then put into a fresh microcentrifuge tube, and a 0.1X volume of 3M sodium acetate (NaAc) added followed by a 3.5X volume of 100% ethanol. The solutions were mixed thoroughly by inversion and the tube microcentrifuged (16,000 x g) for 10 min. The supernatant was discarded and

the pellet washed using 100µl of 70% ethanol. The tube was then centrifuged for a further 1 min, the ethanol removed and the pellet allowed to air dry. Once dry, the pellet was resuspended in 50µl SDW.

The second method was provided by members of the host laboratory. 1.5ml of yeast pre-culture was centrifuged at for 2 min and the pellet resuspended in 250µl STE buffer (100mM Tris-HCl, 50mM EDTA, 500mM NaCl). 25µl of 20% w/v SDS and a scoop of glass beads (<100µl) were added to the tube and then vortexed for 1 min. The tube was incubated for 20 min at 65°C before addition of 90µl of 3M potassium acetate (KAc) with inversion to mix. The tube was then incubated on ice for 15 min and the top layer transferred to a fresh tube. This was then centrifuged for 10 min. The resulting supernatant was transferred to a fresh tube and 800µl 100% ethanol added with inversion to mix. This was then incubated on ice for 10 min, followed by microcentrifugation (16,000 x g) for 10 min. The pellet was then washed using 500µl 70% (v/v) ethanol, centrifuged for 5 min and the ethanol removed. The pellet was allowed to air dry and then was resuspended in 50µl SDW. Genomic DNA samples were stored at -20°C.

2.6 Plasmid minipreps

Plasmid minipreps from *E. coli* were either performed using the PureYield™ Plasmid Miniprep System (Promega) or the following method. A single *E. coli* colony was used to inoculate 2ml of liquid LB amp medium in universal sample tubes and incubated at 37°C overnight with shaking (200RPM). 1ml of the culture was then microcentrifuged (16,000 x g). The

supernatant was discarded and the pellet was resuspended in 200µl of Solution I (50mM glucose, 25mM Tris HCl pH 8.0, 10mM EDTA pH 8.0) by pipetting gently up and down. 200µl of Solution II (0.2M NaOH, 1% w/v SDS) was then added and mixed by inverting thoroughly. 200µl of Solution III (3M potassium acetate to pH 4.8 with acetic acid) was then added and mixed by inverting thoroughly. The cell suspension was then microcentrifuged (16,000 x g) for 5 min. The resulting supernatant was transferred to a fresh microcentrifuge tube, 600µl of 100% (v/v) isopropanol added, and mixed thoroughly by inverting. The tube was then centrifuged for 10 min and the supernatant discarded. 100µl of 70% ethanol was added and centrifuged for a further minute. The ethanol was then removed and the pellet allowed to air dry, before being resuspended in 50µl SDW. Plasmid samples were stored at -20°C.

2.7 Plasmid constructions

Insert DNA was amplified by PCR (primers and template DNA are detailed in *2.3 PCR and Primers*). Correct amplification was verified by gel electrophoresis using 1% Tris-acetate-EDTA (TAE) agarose gel and buffer. If the electrophoresis showed only one correctly sized band, the insert was purified by PCR Clean-up. If more than one band was present, the required band was purified by gel extraction. Inserts and vector were then double digested as required using restriction enzymes from NEB at 37°C (further details in Table 3). Digested vector was purified by gel electrophoresis and extraction, and digested inserts were incubated at 80°C for 20 min to heat

inactivate the restriction enzymes. The vector and insert were ligated together using T4 DNA ligase (NEB) with a molar ratio of 1:3 vector to insert (using 75ng of vector), overnight at 16°C according to manufacturer's instructions. The ligation mix was then electroporated into competent *E. coli* cells using the electroporator setting Ec1 (MicroPulser™, Bio-Rad). Two 10X serial dilutions of the *E. coli* suspension were then made and 1ml of each of the three suspensions spread onto LB Amp agar plates, which were incubated overnight at 37°C. Typically, 12 of the resulting colonies were selected and plasmid extracted according to the protocol detailed earlier in *2.6 Plasmid minipreps*. Plasmids were verified by restriction enzyme digest and gel electrophoresis (Figure 8). All PCR clean-ups and gel extractions were performed using NucleoSpin® Gel and PCR Clean-up (Macherey-Nagel), according to the manufacturers' instructions.

The pRS315-*RAD54*-GFP plasmid was created by ligating the *RAD54* insert into the pRS315 vector to produce the plasmid pRS315-*RAD54*, then ligating the GFP tag insert into pRS315-*RAD54.* The three gene overexpression plasmids (for *CDC73, ADH1* and *GPD1*) were created by ligating a single copy of the gene in question into the pCM190 plasmid (Garí et al. 1997), placing the ORF under the control of a tetracycline regulatable promoter. Plasmid maps are presented in Figure 8.

Table 3. Digestion conditions for inserts and vectors for the production of plasmids used in the project.

Plasmid	Insert	Vector	Restriction enzymes	NEBuffer	Digest time
pRS315-*RAD54*	*RAD54*	pRS315	*Sal*I-HF® and *Xma*I	CutSmart™	1h
pRS315-*RAD54*-GFP	GFP tag	pRS315-*RAD54*	*Xma*I and *Sac*I-HF®	CutSmart™	1h
pCM190-*CDC73*	*CDC73*	pCM190	*Not*I-HF® and *Pst*I	2.1	2h
pCM190-*ADH1*	*ADH1*	pCM190	*Not*I-HF® and *Pst*I	2.1	2h
pCM190-*GPD1*	*GPD1*	pCM190	*Not*I-HF® and *Pst*I	2.1	2h

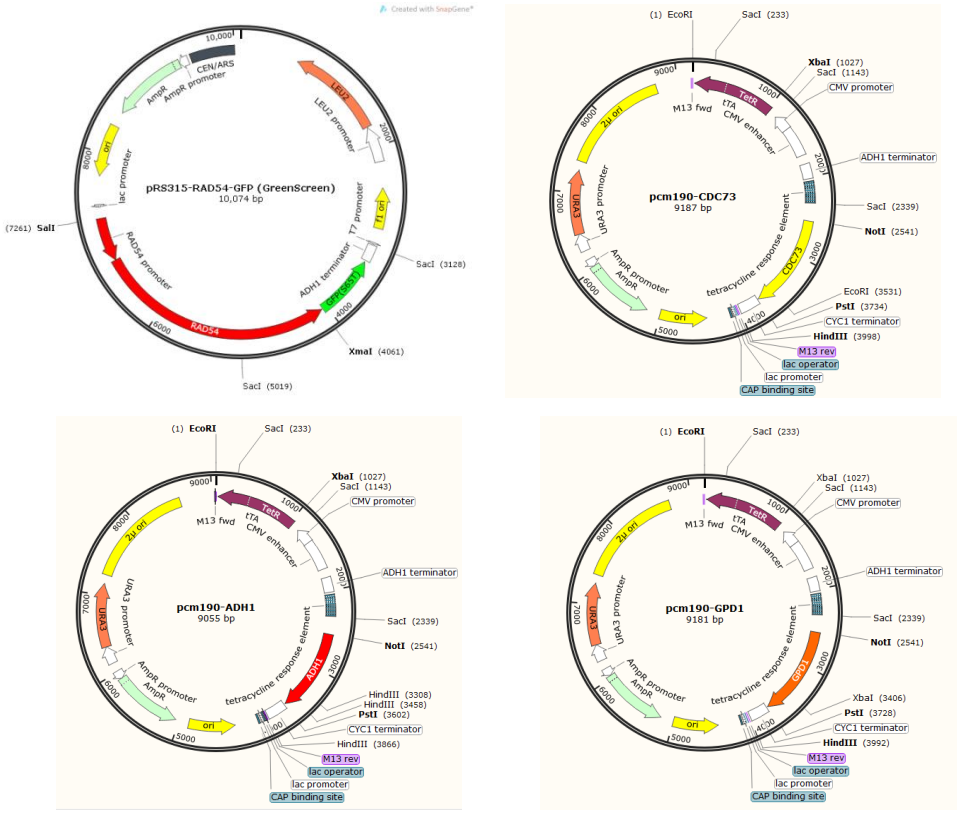


Figure 4. Maps of the four plasmids constructed in this project. Top left: pRS315-RAD54-GFP. Top Right: pCM190-*CDC73*. Bottom left: pCM190-*ADH1*. Bottom right: pCM190-*GPD1* (SnapGene®).

2.8 Yeast Transformations

Yeast pre-cultures were diluted to OD_{600} ~0.5 at a final volume of 25ml in the morning and allowed to recover to at least OD OD_{600} ~2. The full volume of yeast culture was then centrifuged in a 50ml centrifuge tube at 3,100 x g for 5 min. The supernatant was discarded and the pellet washed in 5ml of SDW. 1ml of cells was then centrifuged for 1 min. The supernatant was removed and the pellet resuspended in 1ml 100mM lithium acetate (LiAc). This was then incubated at 30°C for 10 min before centrifugation and the supernatant discarded. The pellet was then covered in a layer of 240µl 50% w/v polyethylene glycol (PEG). 36µl of 1M LiAc, 52µl of denatured SS carrier DNA, and 0.5µg transformation DNA were added to the top of the layer of PEG. The tube was then vortexed until the pellet was completely resuspended. The tube was then incubated at 30°C for 30 min, followed by heat shock at 42°C for 20 min, with occasional vortexing. The cells were then pelleted and resuspended gently in 500µl of SDW. 200µl of the cell suspension were plated onto an appropriate selective medium. Negative controls were performed by replacing the transformation DNA with an equivalent volume of SDW

2.9 Dihydroethidium superoxide assay

Yeast pre-cultures were diluted in the morning to OD_{600} ~0.5. Treated cells then had artesunate stock added to produce a final concentration of 100µM; untreated cells had an equivalent volume of 70% ethanol added. The

cultures were then allowed to recover to at least OD_{600} 2. 1.5ml of OD_{600} ~2 cells were centrifuged and resuspended in 100µl phosphate buffered saline (PBS). Where indicated, DHE stock was added to produce a final concentration of 5µM. An equivalent volume of DMSO was added to a control set of cultures. The tubes were incubated at 30°C for 30 min with shaking (200RPM). The cell suspensions were then centrifuged again and resuspended in 100µl fresh PBS. For microscopic analysis, 10µl of the cell suspension was transferred to a microscope slide and covered with a cover slip, then examined with a fluorescence microscope (GX microscopes, L3201-LED). For flow cytometric analysis, a further 400µl of PBS was added to the cultures to make a final volume of 500µl. Flow cytometry of DHE stained cells was performed using a Beckman Coulter FC500, using the filter FL3 (488nm excitation, 612-638 emission bandwidth), set to take 100,000 counts or run sample for five minutes, whichever occurred first. Flowing Software (version 2.5.1) was used to analyse data. As *cdc73Δ* mutant cells have an enlarged morphology (Jorgensen et al. 2002), relative fluorescence of both mutant and WT were normalised by dividing mean fluorescence by mean forward scatter (FS) of gated populations. Population of brightly fluorescing cells was taken as the percentage of total events represented by the secondary peak visible in stained cells.

2.10 Generation of petite mutants

Petite mutants are mutants which lack the ability to respire aerobically, either through significant damage to the mitochondrial genome or loss of

mitochondria altogether. Petite mutants were produced by selecting four WT colonies and four *cdc73Δ* colonies and spreading them onto a specific quadrant of YEPD agar plates containing 40µg ml^{-1} EtBr. The plates were then incubated at 30°C until new colonies became visible. One colony per quadrant was then spread onto the corresponding quadrant of a second set of YEPD EtBr agar plates and the process repeated. After the yeast had been grown on three sets of EtBr agar plates, the yeast was then spread onto normal YEPD agar plates. The colonies were verified as being petite by inoculating growth media containing only a non-fermentable carbon source and verifying that no growth took place.

2.11 Fermentations

For anaerobic fermentations, yeast pre-culture was diluted to OD_{600} ~0.5 and allowed to recover to OD_{600} ~2. 1ml of this culture was used to inoculate a conical flask containing 50ml of YEPD broth. This was done in triplicate for WT and *cdc73Δ* strains at each of two glucose concentrations (6% and 10% w/v) in the YEPD. The flasks were sealed in an airtight container with an anaerobic Gas-pak™ (Becton, Dickinson and Company). The container was then incubated statically at 30°C for five days.

For aerobic fermentations, 10ml yeast pre-cultures were allowed to grow to saturation. This 10ml was then used to inoculate 1 litre of YEPD containing 6% glucose w/v. The culture was allowed to grow overnight at 30°C with shaking (20RPM). The culture was centrifuged at 3,600 x g for 10 min and the pellet weighed. The pellet was resuspended at 50% w/v in

reverse osmosis (RO) water to form a cell slurry. A 1ml sample of the slurry was diluted to establish the cell density using a haemocytometer, allowing appropriate inoculation of 15 fermentation vessels containing 100ml YEPD 6% glucose w/v and stirrer bars to achieve a starting concentration of 10^7 cells ml^{-1}. The fermentation flasks were sealed and fitted with a valve to allow CO_2 release. The weight of the flasks was measured immediately after sealing. The flasks were then incubated at 30°C with stirring at 250RPM. The flasks were periodically weighed over the next 96 h. At each of five time points (20, 26, 48, 72 and 96 h) three of the fifteen flasks were removed after weighing for analysis. Cell counts were taken at 26, 48 and 72 h. Samples were stained by adding 100µl of yeast culture to 100µl of methylene blue solution (0.5% w/v) and 800µl SDW then vortexed in a microcentrifuge tube to enumerate viable cells using a haemocytometer. Media samples were transferred into 50ml centrifuge tubes and centrifuging at 3,100 x g for 5 min. The supernatants were then collected and filtered using a 0.45µM filter to remove any cells, dissolved gas, or other debris. The supernatant was analysed using a density meter and an alcohol meter (DMA 4500 and Alcolyzer Plus respectively, Anton Paar). A blank measurement was also taken of uninoculated medium and subtracted from all values.

2.12 Spotting assays

Yeast pre-cultures were diluted to OD_{600} ~0.5 and allowed to recover to at least OD_{600} 2. They were then diluted to OD_{600} ~2. 1ml of culture was centrifuged, the supernatant discarded, and the pellet resuspended in

phosphate buffered saline (PBS). Serial decimal dilutions of the suspension were prepared (down to 10^{-4}). Medium for spotting assays was prepared by melting agar medium and incubation in a 50°C water bath before adding artesunate stock solution to achieve the required final artesunate concentration. The medium was mixed gently by inverting to minimise bubble formation, then quickly distributed either into 60mm petri dishes (7.5ml per dish) or individual wells of a 48-well plate (300µl per well). Cell suspensions were vortexed just prior to spotting to ensure even cell distributions. Cell suspensions were spotted onto solidified medium at a volume of 3µl per spot. Spotting assays were incubated at 30°C until colonies could be counted. This was usually after 2 d for aerobic cultures and 7 d for anaerobic cultures.

2.13 Assay for *RAD54-GFP* activation

The yeast gene *RAD54* is known to be up-regulated when yeast cells are exposed to genotoxins and this property can be exploited as a bioreporter of genotoxicity. This is informally referred to as a GreenScreen® assay (Cahill et al. 2004). Two methods were used to fuse a GFP tag onto Rad54p, one by incorporating the fusion into the yeast genome and the other by expressing the fusion protein from a plasmid. The plasmid-borne *RAD54*-GFP fusion cassette described above was PCR amplified with the *RAD54*-GFP fusion primers from the plasmid pFA6a-GFP(S65T)-His3MX6 (Table 2) to produce a DNA insert that would integrate a GFP tag and a His marker into the yeast genome via homologous recombination at the native *RAD54* locus, i.e. short-flanking homology PCR (Longtine et al. 1998). Accordingly the amplified

insert was purified by gel extraction, and then transformed into haploid yeast strain BY4741 (as detailed in *2.4 Yeast transformations*). The gene map of the fusion protein is depicted in Figure 5. Both *RAD54*-GFP fusion yeast and yeast transformed with the pRS315-*RAD54*-GFP plasmid were prepared in the same way. Yeast pre cultures were diluted to OD_{600} ~0.5 in YEPG for artesunate treatment and YEPD for paraquat or EtBr as positive controls. These agents were added to the cultures to final concentrations of 5µM artesunate, 0.15mM paraquat or 0.016mM EtBr. The cultures were allowed to recover to OD_{600} ~2 and then prepared for either microscopic analysis (as described above) or flow cytometry. 1.5ml of cell suspension was centrifuged and resuspended in 100µl of PBS. For flow cytometry, a further 400µl of PBS was added to the cultures to make a final volume of 500µl. Flow cytometric analysis was performed using a Beckman Coulter FC500, using the filter FL1 (488nm excitation, 514-542nm emission bandwidth), set to take 100,000 counts or run sample for five minutes, whichever occurs first. Flowing Software (version 2.5.1) was used to analyse data.

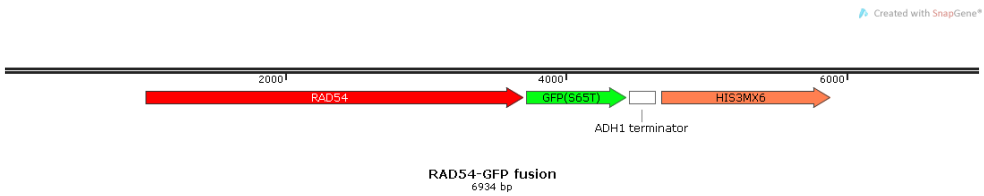


Figure 5. Map of RAD54-GFP fusion protein sequence. *S. cerevisiae* native *RAD54*, fused to GFP sequence, *ADH1* terminator sequence and Histidine marker HIS3MX6 (SnapGene®).

3. Results

3.1 Artesunate inhibits growth of yeast on both fermentable and non-fermentable carbon sources

Growth curves of wild type *S. cerevisiae* were produced on both YEPD and YEPG media using varying concentrations of artesunate, to establish appropriate inhibitory concentrations to use throughout the project (Figure 6A, B). On YEPD, concentrations ranging from 0.125mM to 8mM were tested, and it was decided that concentrations between 1 and 8mM would be suitable for screening. When grown on the glycerol-based medium, it was apparent that the yeast was far more sensitive to artesunate. A range of 1µM to 10µM was selected for screening purposes.

When grown media containing low glucose concentrations, it is possible to see a point where the yeast growth rate changes, known as the diauxic shift. The shift appears as a second lag plus exponential phase. It is known to occur when the glucose supply in the medium becomes exhausted and the yeast begins utilising the ethanol in the medium as a carbon source for aerobic respiration, the ethanol having been secreted as a by-product of glucose catabolism (Galdieri et al. 2010). Growth curves were also produced using YEPD containing 0.5 and 0.1% glucose, to bring forward and accentuate the diauxic shift. Effects of artesunate on growth are largely apparent only after the diauxic shift, suggesting that respiratory growth is the artesunate sensitive phase (Figure 6C, D).

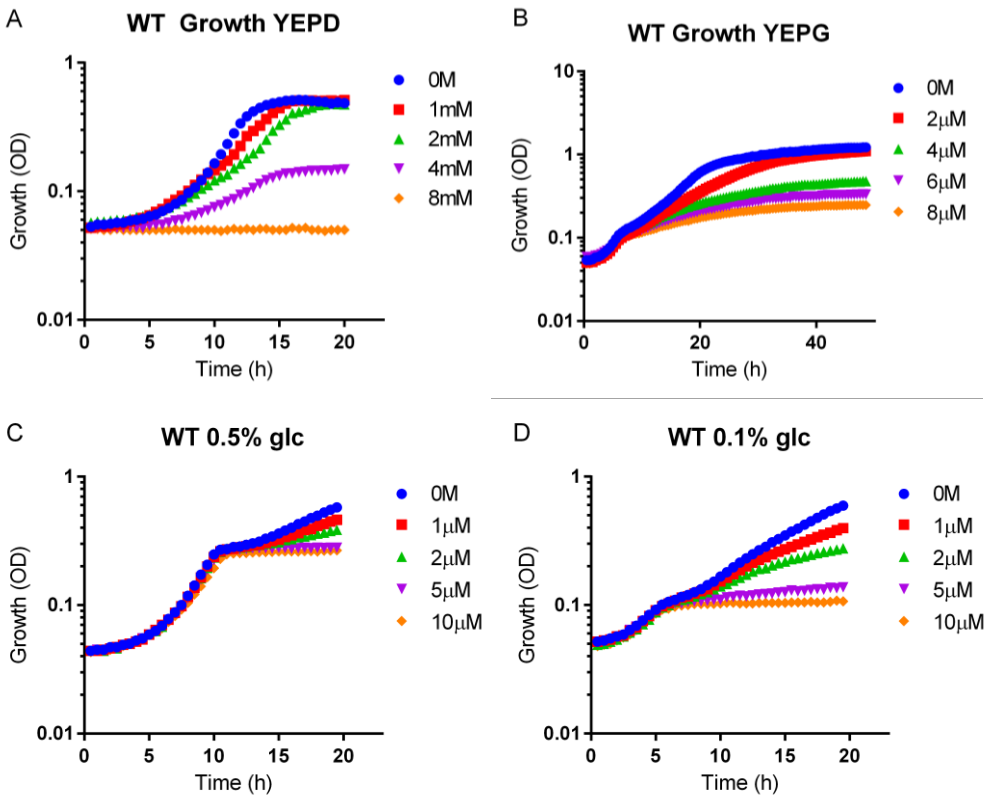


Figure 6. WT growth curves. (A) Growth curves of WT (BY4743) *S. cerevisiae* on YEPD medium with a range of concentrations of artesunate. (B) Growth curves of WT *S. cerevisiae* on YEPG medium (including 0.1% glucose w/v) with a range of concentrations of artesunate. (C, D) Growth curves of WT *S. cerevisiae* on YEPD medium containing 0.5% and 0.1% glucose respectively. The inset symbol legends refer to artesunate concentrations. Note: all growth curves shown are single representative experiments from one of at least three independent replicates. Reported trends were consistent from experiment to experiment, although absolute growth rates varied between independent experiments for reasons outside our control. This complicated averaging of the data.

3.2 The yeast deletion mutant *cdc73Δ* shows increased sensitivity to artesunate on YEPD medium

A large scale screen for artesunate sensitivity against the entire set of homozygous deletion mutants from the Yeast Deletion Collection (Winzeler et al. 2009) was performed by other members of the Avery laboratory prior to the start of the project (Tindall S, Vallieres C, Avery SV, unpublished data). Twenty one mutants with related functions that had shown possible

phenotypes from within this screen were chosen to be the starting point of this project. Seven deletion mutants were for genes involved in DNA mismatch repair (MMR). Fourteen deletion mutants were for genes with telomere-related functions (for complete list of genes and their functions, see Table 4 in *6. Appendix*). The mutants were all tested individually for artesunate sensitivity on both YEPD and YEPG. Of the initial 21 mutants, only one exhibited a clear phenotype. On YEPD medium, WT yeast showed slight inhibition in the presence of 1mM artesunate, but growth of *cdc73Δ* cells was strongly inhibited (Figure 7A). This increased sensitivity of the *cdc73Δ* cells was not present on YEPG medium (data not shown). The *cdc73Δ* mutant was tested individually with 10 to 100µM artesunate to verify the phenotype (see Figure 7B for 100µM artesunate). The cell doubling times were calculated from the growth curves over this range of artesunate concentrations, and showed a gradual slowing of growth between 0–100µM artesunate in the mutant whereas the WT was unaffected (Figure 7C). Along with its increased artesunate sensitivity (two-way ANOVA of doubling time 0M vs 100µM, WT p=0.5162, *cdc73Δ* p=0.0010). Growth curves for the other 20 mutants (not shown) were similar to WT.

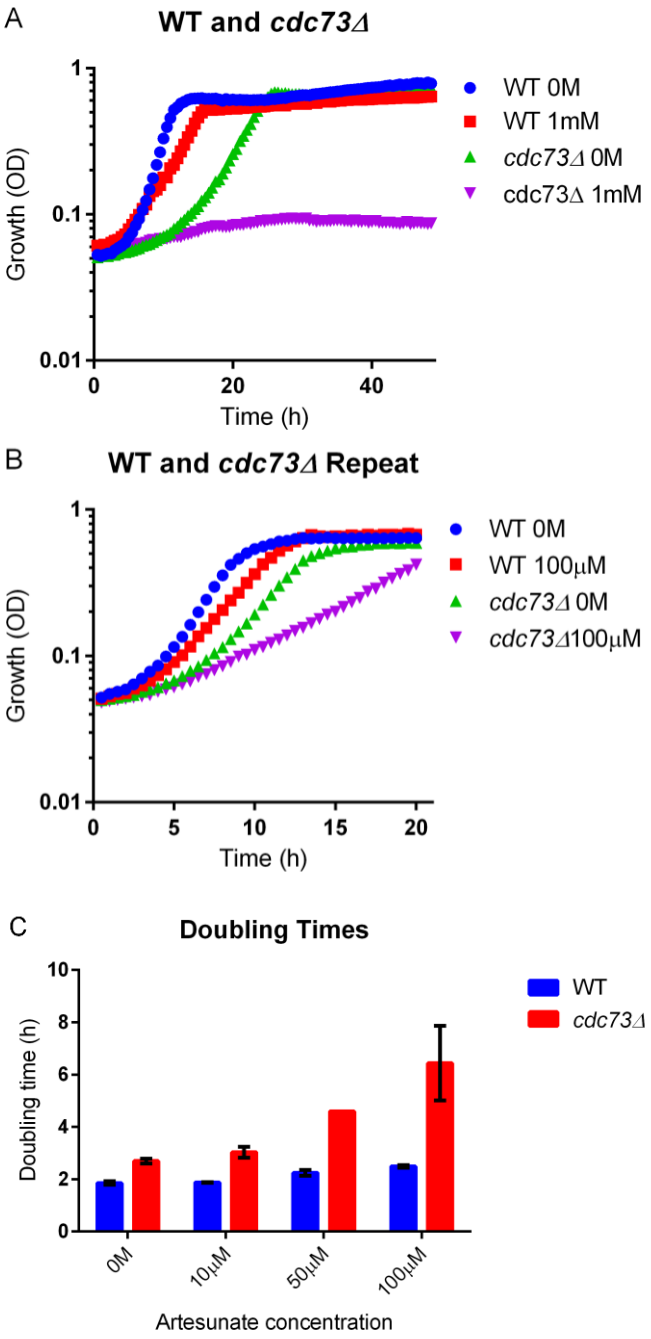


Figure 7. WT and *cdc73Δ* yeast growth curves and doubling times. (A) WT and *cdc73Δ* yeast growth curves in YEPD, in the presence and absence of 1mM artesunate. (B) WT and *cdc73Δ* yeast growth curves in YEPD, in the absence and presence of 100µM artesunate. (C) Effect of artesunate on the doubling times of WT and cdc73Δ, derived from Figure 7B and other growth curves (not shown). Mean values from two independent replicates are shown +/- SEM. Note that cdc73Δ mutant at 50µM lacks error bars as the other replicates became contaminated. Growth curves are of single representative experiments (see Note in legend to Figure 6).

3.3 Overexpression of *CDC73* in a WT background does not affect artesunate sensitivity

Gene overexpression is a useful tool for identifying drug targets (Prelich 2012). If the encoded protein is a direct target of a drug, then increasing its abundance can often confer some resistance to the host cell. Phenotypes arising from gene deletion are less specific to the normal target (Avery 2011). Overexpression of *CDC73* was achieved in WT cells by transforming them with the plasmid pCM190-*CDC73* (details in *2.7 Plasmid constructions* and Figure 4, plasmid verified by restriction digest, Figure 8A). Overexpressing *CDC73* did slightly increase the doubling time of the yeast but had no marked effect on the sensitivity to artesunate relative to minus-artesunate control growth (Figure 9B). These results are consistent with existing research that overexpressing *CDC73* will slow growth rate (Sopko et al. 2010). This suggests that Cdc73p is not a direct target of artesunate, but that its presence is required for normal artesunate resistance.

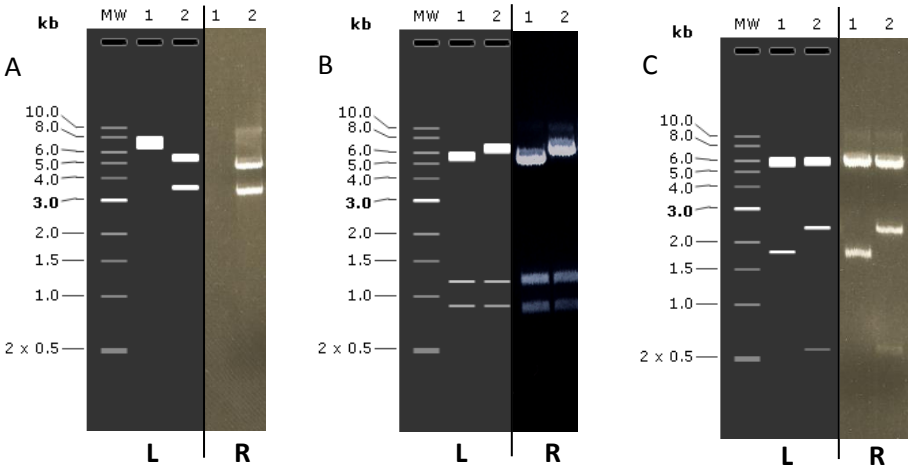


Figure 8. Gel verification of overexpression plasmid constructs. Left (L) is a SnapGene® (GSL Biotech) simulation of expected banding pattern; Right (R) is actual banding pattern. Lane 1 is unaltered pCM190; Lane 2 is pCM190 with inserted gene. (A) pCM190-*CDC73* digested with *Eco*RI. NB pCM190 missing from lane 1 (B) pCM190-*ADH1* digested with *Sac*I. (C) pCM190-*GPD1* digested with *Xba*I and *Hind*III.

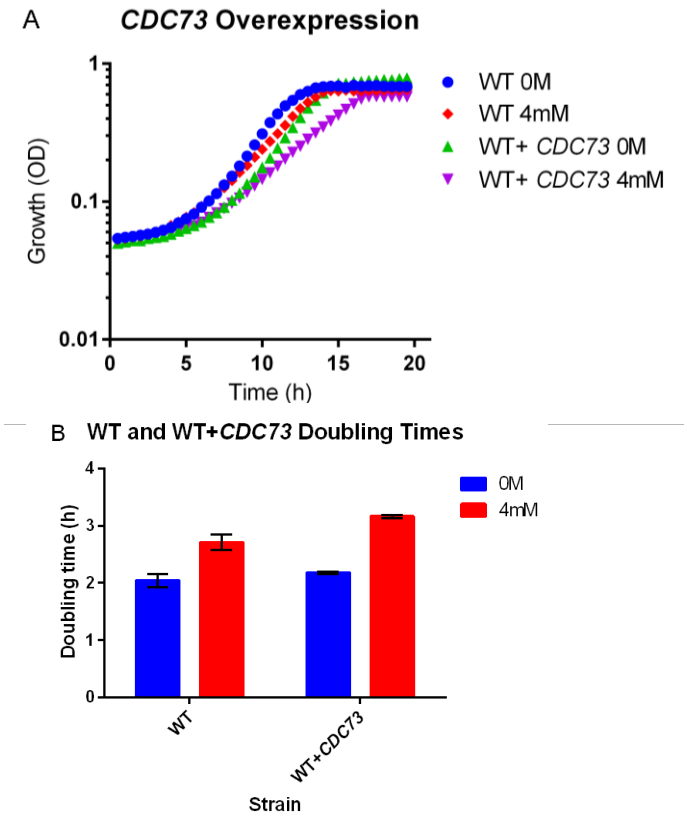


Figure 9. WT and *cdc73Δ* cell growth curves and doubling times of *CDC73* overexpression in WT. (A) Growth curves in YEPD of WT cells and the same organism transformed with *CDC73* overexpression plasmid pCM190-*CDC73* (WT+*CDC73*) In YEPD, in the presence and absence of 4mM artesunate. Plasmid rescue was performed on WT+*CDC73* yeast to ensure correct transformation, but Cdc73p concentration was not directly measured. Growth curves are of single representative experiments (see Note in legend to Figure 6). (B) Mean doubling times of WT and WT+*CDC73* in YEPD, in the presence and absence of 4mM artesunate +/- SEM.

3.4 The deletion mutants *leo1Δ*, *rtf1Δ*, *pdc1Δ*, *pdc5Δ* and *pdc6Δ* do not show increased sensitivity to artesunate on YEPD medium

In normal yeast cells, Cdc73p forms part of the Paf1p protein complex. The Paf1 complex has diverse functions in yeast, including regulation of gene expression, gene silencing and cell cycle progression. The complex is also conserved in higher eukaryotes (Tomson and Arndt 2013). Along with Cdc73p, four other proteins make up the complex, Paf1p, Leo1p, Rtf1p, and Ctr9p. Because of their link with Cdc73p, it was decided to test deletion mutants in the corresponding genes for artesunate sensitivity. Only *leo1Δ* and *rtf1Δ* were successfully tested as *paf1Δ* failed to grow once thawed from -80°C stocks and *ctr9Δ* is not present in the deletion library. Both mutants showed a slower than normal lag phase, similar to the *cdc73Δ* cells, and also a slight increase in sensitivity to the drug, but not to the extent seen in the *cdc73Δ* mutant (Figure 10).

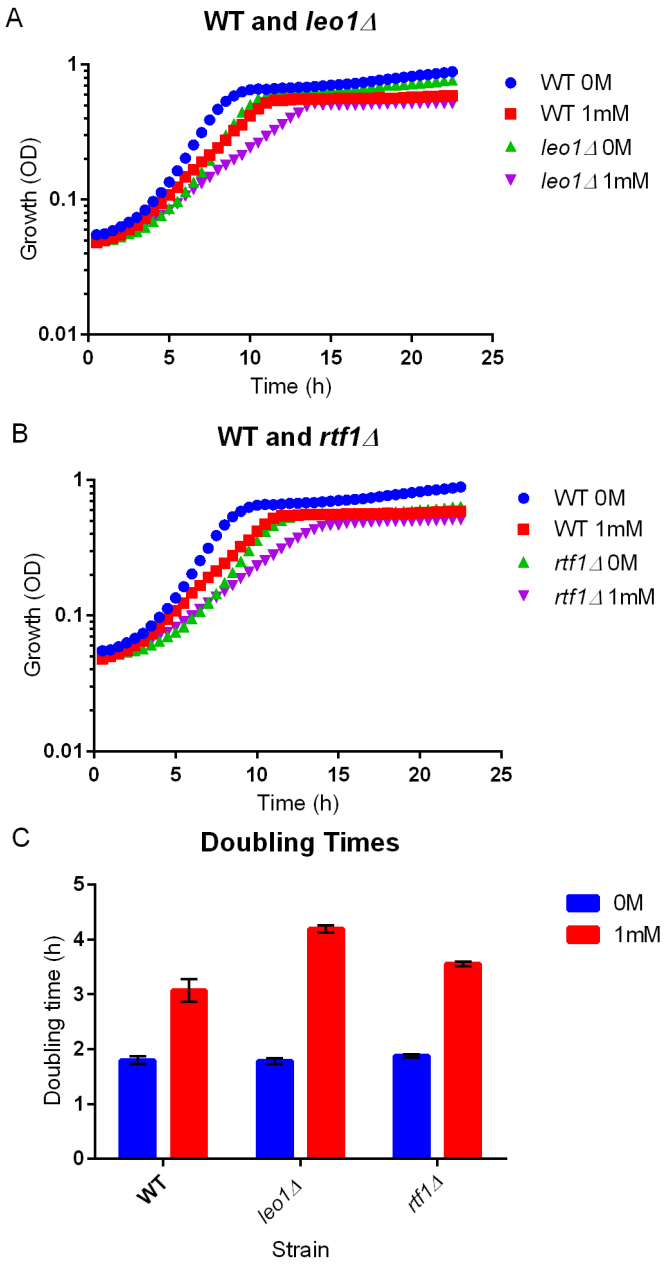


Figure 10. WT, and *leo1Δ* and *rtf1Δ* deletion mutant growth curves (A) Growth curves in YEPD of WT and *leo1Δ* mutant *S. cerevisiae* in the absence and presence of 1mM artesunate. Growth curves are of single representative experiments (see Note in legend to Figure 6). (B) Growth curves in YEPD of WT and *rtf1Δ* mutant *S. cerevisiae* in the absence and presence of 1mM artesunate. (C) Mean doubling times of WT, *leo1Δ*, and *rtf1Δ S. cerevisiae* in YEPD, in the presence and absence of 1mM artesunate +/- SEM.

As artesunate sensitivity of the *cdc73Δ* mutant only manifested itself when it was cultured on YEPD, it was suspected that a key target of the drug could be located in the fermentation pathway and which may become susceptible to damage from artesunate when Cdc73p is absent. The fermentation pathway is only active in the presence of high concentrations of glucose. The first stage of this pathway is the conversion of pyruvate to acetaldehyde. The process is catalysed by three isozymes of pyruvate decarboxylase (PDC) (Kellermann et al. 1986, Seeboth et al 1990, Hohmann 1991). The deletion mutants of these genes (*pdc1Δ*, *pdc5Δ*, *pdc6Δ*) were tested for artesunate sensitivity. None expressed a phenotype different from the WT, resulting in nearly identical growth curves in the absence and presence of artesunate (Figure 11). This indicated that each of these genes' functions are not involved in normal artesunate resistance, although the possibility of redundancy and a role for total pyruvate decarboxylase activity cannot be ruled out. During this experiment, abnormally high inhibition at 1mM artesunate was observed. As this is present in both WT and each of the mutants, this was likely due to an artesunate stock concentration error.

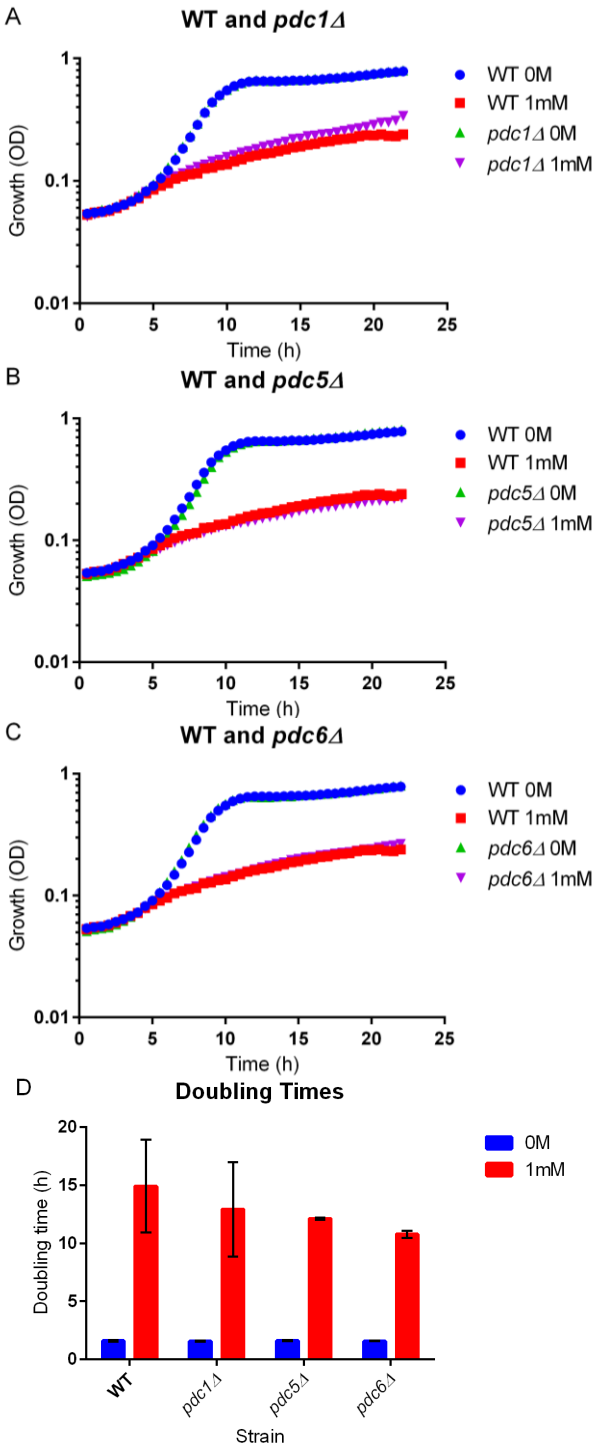


Figure 11. WT and pyruvate decarboxylase mutant growth curves. (A, B, C) Growth curves in YEPD of WT *S. cerevisiae* and three pyruvate decarboxylase mutants (*pdc1, 5, 6Δ*) in the absence and presence of 1mM artesunate. Growth curves are of single representative experiments (see Note in legend to Figure 6). (D) Mean doubling times of WT and PDC mutants in YEPD, in presence and absence of 1mM artesunate +/- SEM.

3.5 The *cdc73Δ* mutant shows higher intracellular reactive oxygen species than WT when grown on YEPD

Previous research indicates that artesunate causes cell damage via the generation of reactive oxygen species (ROS) (Wang et al. 2010). WT and *cdc73Δ* cells were assayed for ROS using the superoxide indicator dihydroethidium (DHE), which fluoresces red when oxidised.

Preliminary results for untreated cells were obtained using fluorescence microscopy. In both WT and *cdc73Δ* strains, a small sub-population of cells fluoresced bright red, while the rest of the population showed faint red fluorescence. The proportion of bright fluorescing cells appeared considerably higher in *cdc73Δ* than the WT cells (Figure 12).

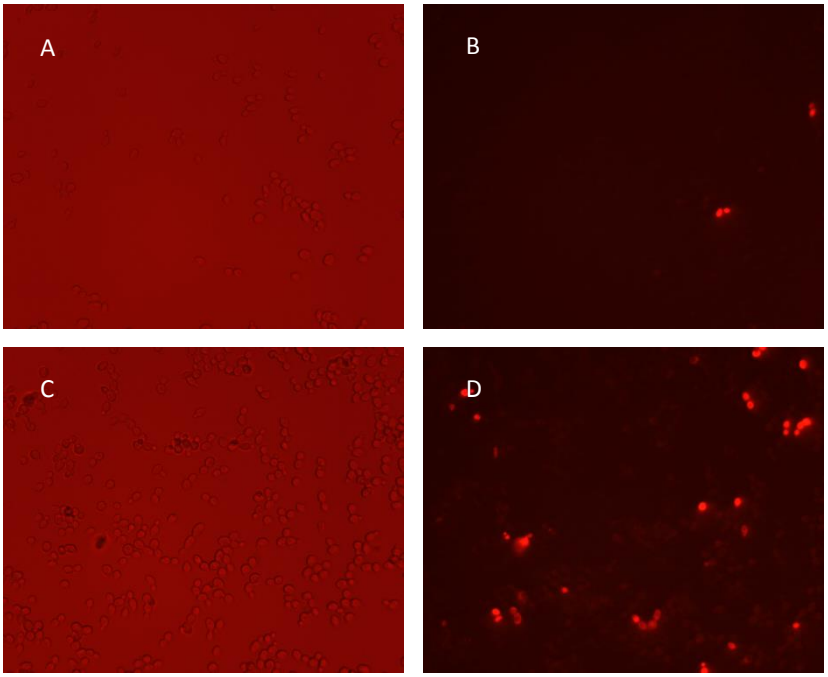


Figure 12. Microscopic analysis of DHE staining. Yeast cells stained with dihydroethidium at 400x magnification. (A) WT cells under normal light, 6ms exposure. (B) WT cells under blue light, 350ms exposure. (C) *cdc73Δ* cells under normal light, 6ms exposure. (D) *cdc73Δ* cells under blue light, 350ms exposure.

In order to quantify the subpopulations, they were analysed by flow cytometry. The brightly fluorescent cell subpopulation was evident as a second peak in fluorescence histograms (Figure 13A). In the case of mean fluorescence of cells not in the brightly fluorescing sub-population, *cdc73Δ* cells showed higher DHE staining than WT cells (Figure 13B) and this was reflected also when the brightly fluorescing subpopulations were considered as a proportion of the total culture (Figure 13C). The data indicate that the *cdc73Δ* mutant has higher intracellular superoxide levels than WT. Neither method of analysis indicated an increase in superoxide levels following artesunate treatment of either strain. However, a decrease in DHE-staining seen in artesunate-treated WT cells was not evident with the *cdc73Δ* mutant (Figure 13B, C).

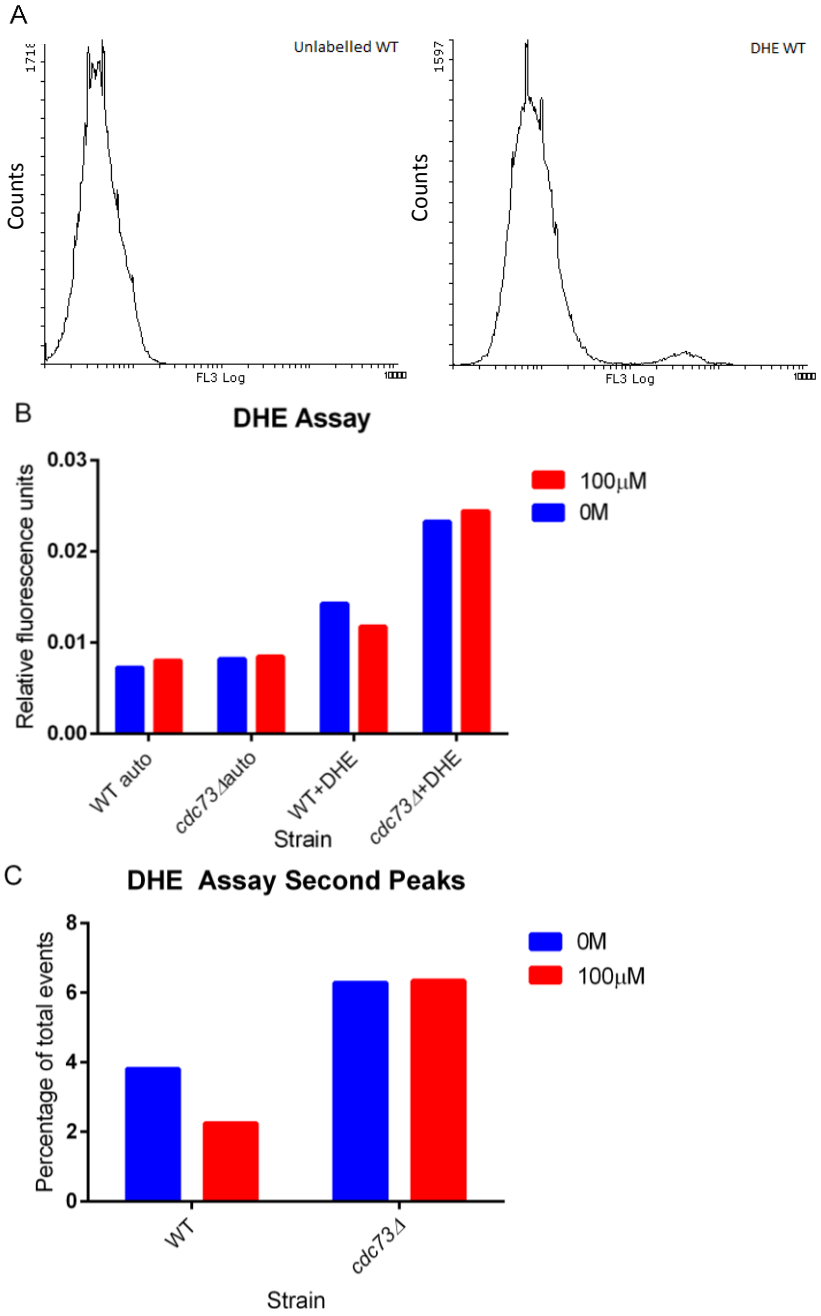


Figure 13. Flow cytometric analysis of DHE staining. (A) Flow cytometry histograms of WT yeast, unlabelled and labelled with DHE (minus artesunate in both cases). The second (smaller) peak in the right hand histogram was used to calculate the percentage of brightly fluorescing cells. (B) Mean fluorescence of WT and *cdc73Δ* yeast cultures with and without artesunate treatment as measured by flow cytometry. 'Auto' cells were unlabelled; 'DHE' cells were stained with dihydroethidium. (C) Percentage of brightly fluorescing (second peak) cells within WT and *cdc73Δ* cultures stained with DHE, with and without artesunate treatment. Artesunate treatment was 100µM for ~5 h, in YEPD medium.

3.6 Artesunate may not be genotoxic

In the Avery laboratory, it was shown that deletion of certain genes involved in oxidative stress resistance would sensitise yeast to artesunate, in particular *OGG1* which encodes 8-OxoGuanine Glycosylase, which repairs oxidative damage to mitochondrial DNA (Singh et al. 2001). This lead to the hypothesis that artesunate may be genotoxic. Expression of *RAD54* can be used as a bioreporter of genotoxicity (Cahill et al. 2004), so the first attempt at a genotoxicity assay was done by fusing a GFP tag to the 3' end of *RAD54* within the yeast genome and analysing GFP production using fluorescence microscopy. Haploid WT cells either transformed or not with the fusion construct were treated with known genotoxins paraquat and EtBr as well as artesunate and compared with untreated cells. None of the strains or treatments produced any visible fluorescence (data not shown). In a second attempt, the Rad54-GFP protein was expressed from a plasmid (pRS315-*RAD54*-GFP). These results were analysed using flow cytometry to quantify relative fluorescence. The cells used were diploid WT transformed or not with the pRS315-*RAD54*-GFP plasmid. The samples were treated in the same way as the first assay. Treatment with artesunate did not affect the fluorescence of the cells. Treatment with paraquat and EtBr caused a slight increase in fluorescence in both the WT and pRS315-*RAD54*-GFP transformed cells (Figure 14). This shows that treatment with artesunate may not induce the expression of *RAD54*, although the fact that both transformed and

untransformed cells showed increased fluorescence with the positive controls meant that the results could not be regarded as conclusive.

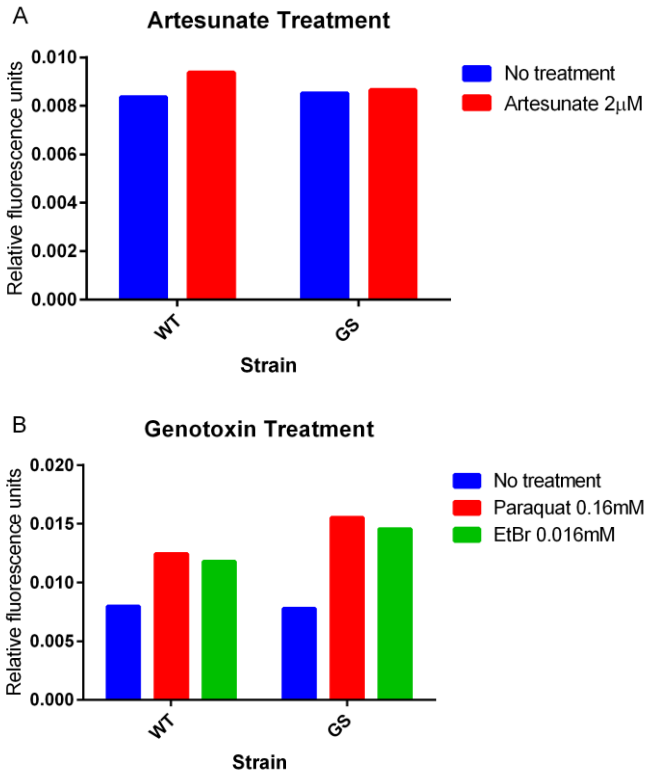


Figure 14. Flow cytometric analysis of genotoxicity assay. (A) Relative fluorescence of two strains of *S. cerevisiae*, grown in YEPG with and without ~5 h 2µM artesunate treatment. (B) Relative fluorescence of two strains of *S. cerevisiae*, grown in YEPG with either no treatment (blue), ~5 h 0.16mM paraquat (red) or ~5 h 0.016mM EtBr (green). 'WT' refers to untransformed wild type cells, 'GS' refers to wild type cells transformed with pRS315-*RAD54*-GFP plasmid.

3.7 Comparison of WT and *cdc73Δ* yeast growth pre- and post-diauxic shift

To compare the fermentative and respiratory growth phases of WT and *cdc73Δ* cells, cultures were prepared in YEPD containing 1%, 0.5%, and 0.1% (w/v) glucose, and allowed to grow for 48 h in order to induce diauxic shift. The graphs produced showed the WT yeast growing as expected, with two distinct growth phases (Figure 15A). However the *cdc73Δ* mutant only showed the first growth phase, with no detectable diauxic shift accompanied by further growth (Figure 15B). This suggested that either *cdc73Δ* cells were defective for ethanol production from the fermentative growth phase (i.e., no alternative, respiratory carbon source produced to support post-diauxic growth), or they cannot utilise ethanol as a carbon source. To resolve these alternative explanations, ethanol was added to the medium. The resultant curves produced by WT and *cdc73Δ* cells both showed post-diauxic growth (Figure 15C, D). This implied that the *cdc73Δ* mutant was defective itself for ethanol production, at least in sufficient quantities to cause a second growth phase.

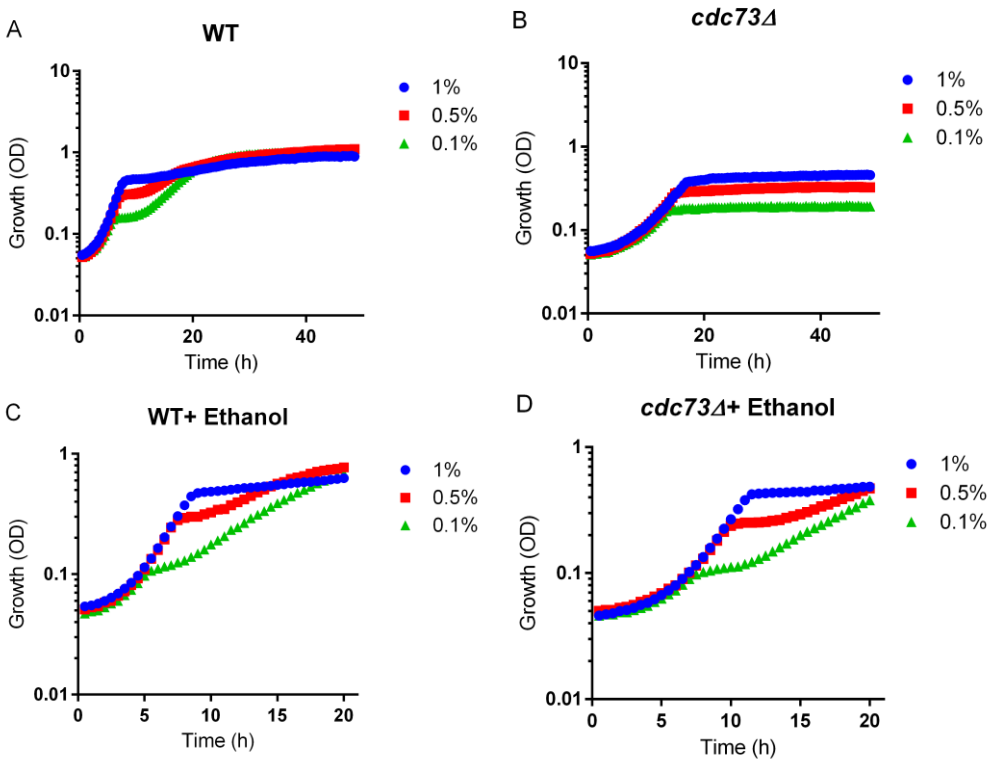


Figure 15. WT and *cdc73Δ* yeast diauxie growth curves. (A, B) WT and *cdc73Δ* yeast growth curves in YEPD containing 1, 0.5 and 0.1% (w/v) glucose. (C, D) WT and *cdc73Δ* yeast growth curves in YEPD containing 1, 0.5 and 0.1% glucose, plus additional 1% (v/v) ethanol. Growth curves are of single representative experiments (see Note in legend to Figure 6).

3.8 Petite mutants of WT and *cdc73Δ* cells show increased sensitivity to artesunate on YEPD medium

If the *cdc73Δ* mutant is unable to synthesise ethanol, this presents a biochemical problem for the cells. In order to produce ATP from glucose, the glycolytic pathway requires a supply of oxidised nicotinamide adenine dinucleotide (NAD^+). NAD^+ is a coenzyme that becomes reduced to form NADH during glycolysis. In aerobically respiring organisms, NADH is re-oxidised during oxidative phosphorylation in the mitochondria. Yeast however can re-oxidise NADH in the final stage of ethanol synthesis (De Smidt et al. 2008). Since the latter stages of aerobic respiration are repressed by the

presence of glucose (Santangelo 2006), if the *cdc73Δ* mutant is not producing ethanol then it would be unclear how it is regenerating NAD^+. Literature exists that states that yeast can counter an NAD^+: NADH imbalance by up-regulating the glycerol production pathway which will regenerate NAD^+ (Bakker et al. 2006). If *cdc73Δ* cells were producing increased levels of glycerol to re-oxidise NADH, there would be a respiratory carbon source present in the medium after glucose exhaustion and we would expect to see a diauxic shift. In aerobically respiring yeast, the stage of oxidative phosphorylation that regenerates NAD^+ is performed by NADH dehydrogenase enzymes (Bakker et al. 2006). These enzymes are in fact also thought to be the point of activation of artemisinins (Li et al. 2005). Their deletion mutants (*nde1Δ* and *ndi1Δ*) both show increased resistance to artemisinin when grown on respiratory media. Considering the present results, it was hypothesized that these enzymes could be inappropriately active in fermenting *cdc73Δ* cells. This would explain how the mutant is regenerating NAD^+ and also why it shows increased sensitivity to artesunate (activated by NADH dehydrogenase) but only on fermentable media.

To test this, petite (ρ-) mutants of WT and *cdc73Δ* cells were generated. Petite mutants either have non-functional mitochondria or lack them altogether and so can only survive on media containing a fermentable carbon source (Goldring et al. 1971). Nde1p and Ndi1p are localised in the mitochondria (Li et al. 2006), and so if their activity is necessary for *cdc73Δ* cells to survive, then a *cdc73Δ*ρ- mutant should be inviable. WT and *cdc73Δ*

strains were treated with EtBr to induce petite mutation. When the resulting strains were grown on media containing only a non-fermentable carbon source they were unable to grow, verifying their loss of respiratory ability. This indicated that the *cdc73Δ* mutant has an alternative means of regenerating NAD^+. Regarding whether artesunate was being activated by Nde1p and/or Ndi1p activity in fermenting *cdc73Δ* cells, it was tested whether the petite mutant may confer some resistance to artesunate. The petite variants of WT and *cdc73Δ* strains were tested for artesunate sensitivity and compared with their non-petite backgrounds. Rather than conferring resistance, the petites actually became slightly sensitised to the drug, with slower growth rates in the presence of artesunate than their corresponding non-petites (Figure 16). This indicates that functional mitochondria are required for normal artesunate resistance on YEPD. The slower growth rate of both petite variants in the absence of artesunate also implies that mitochondria may play a role in normal yeast fermentation.

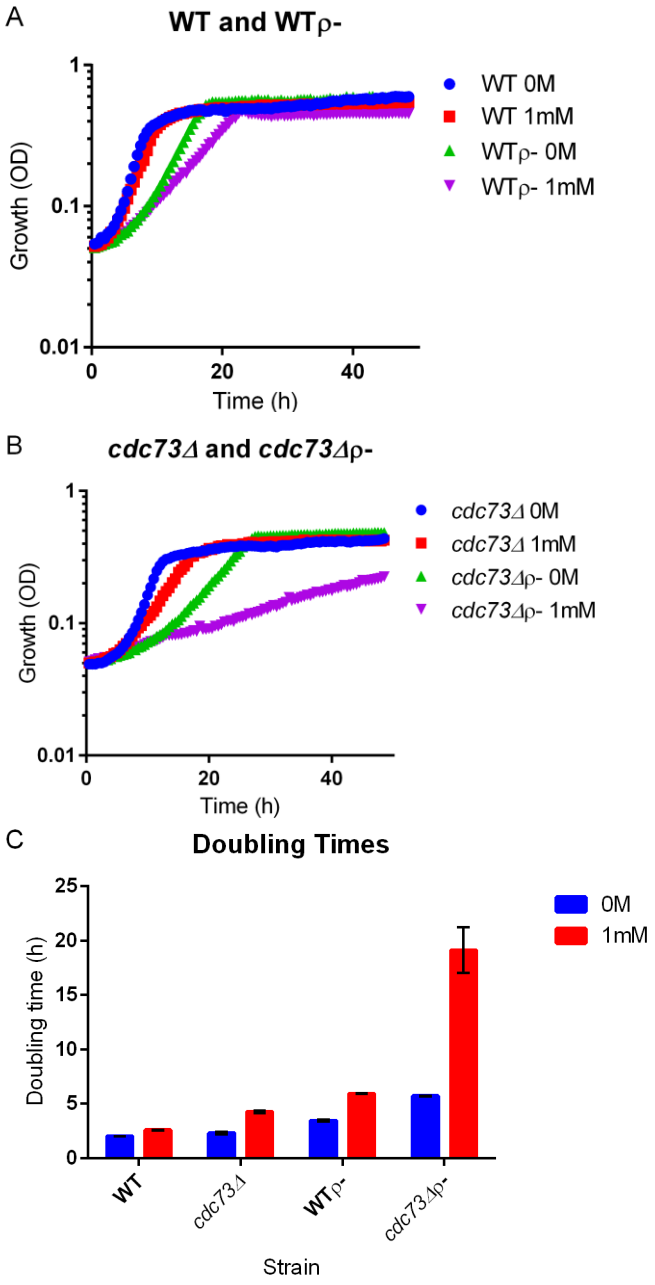


Figure 16. WT and *cdc73Δ* yeast and their petite variants growth curves. (A) WT and WT petite (WTρ-) growth curves on YEPD in the presence and absence of 1mM artesunate. (B) *cdc73Δ* and *cdc73Δ* petite (*cdc73Δ*ρ-) growth curves on YEPD in the presence and absence of 1mM artesunate. Growth curves are of single representative experiments (see Note in legend to Figure 6). (C) Mean doubling times of WT, *cdc73Δ*, and their petite equivalents in YEPD, in the presence and absence of 1mM artesunate +/- SEM.

3.9 The *cdc73Δ* mutant is capable of ethanol production

As the lack of ethanol production in *cdc73Δ* cells had initially been inferred only by the lack of diauxic shift in its growth curves, the ethanol content of the medium during yeast growth was measured directly. Ethanol production by WT and *cdc73Δ* cells was measured using facilities available at the School of Biosciences, Sutton Bonington campus. Accordingly, the yeast growth regime needed to be adapted slightly to match the practices used in Biosciences. Preliminary static cultures of WT and *cdc73Δ* yeast were set up under anaerobic conditions to prevent any catabolism of ethanol. The cultures were also prepared in YEPD containing 6% and 10% glucose w/v to ensure sufficient alcohol production so as to be in the detectable range of the alcohol meter. The initial analyses of ethanol content in the medium supported the hypothesis that *cdc73Δ* cells produce less ethanol than WT cells (unpaired t-test WT vs *cdc73Δ* 6% glucose YEPD p=0.0012 and 10% glucose p=0.0013) (Figure 17A).

Ethanol production over time in aerobic cultures was then measured. Due to the number of flasks involved in the experiment, it was only possible to perform one replicate of the experiment. Weight loss via CO_2 production over time was used as a measure of fermentation activity. Ethanol content of the medium was measured using an alcohol meter. Weight loss and ethanol accumulation occurred less rapidly in the medium with *cdc73Δ* cells, although the final weight (as a percentage of starting weight) and final ethanol concentration in the medium was the same for both WT and *cdc73Δ* cultures

(Figure 17B, C). When ethanol production was corrected for the number of viable cells, which were counted after methylene blue staining at intervals (not shown), the apparent results were reversed with *cdc73Δ* cells producing slightly more ethanol than WT ones. This argued against the hypothesis that the *cdc73Δ* mutant is deficient for ethanol synthesis. The fact that the *cdc73Δ* mutant produces ethanol also indicated that it is not likely to be suffering from an NAD^+: NADH imbalance.

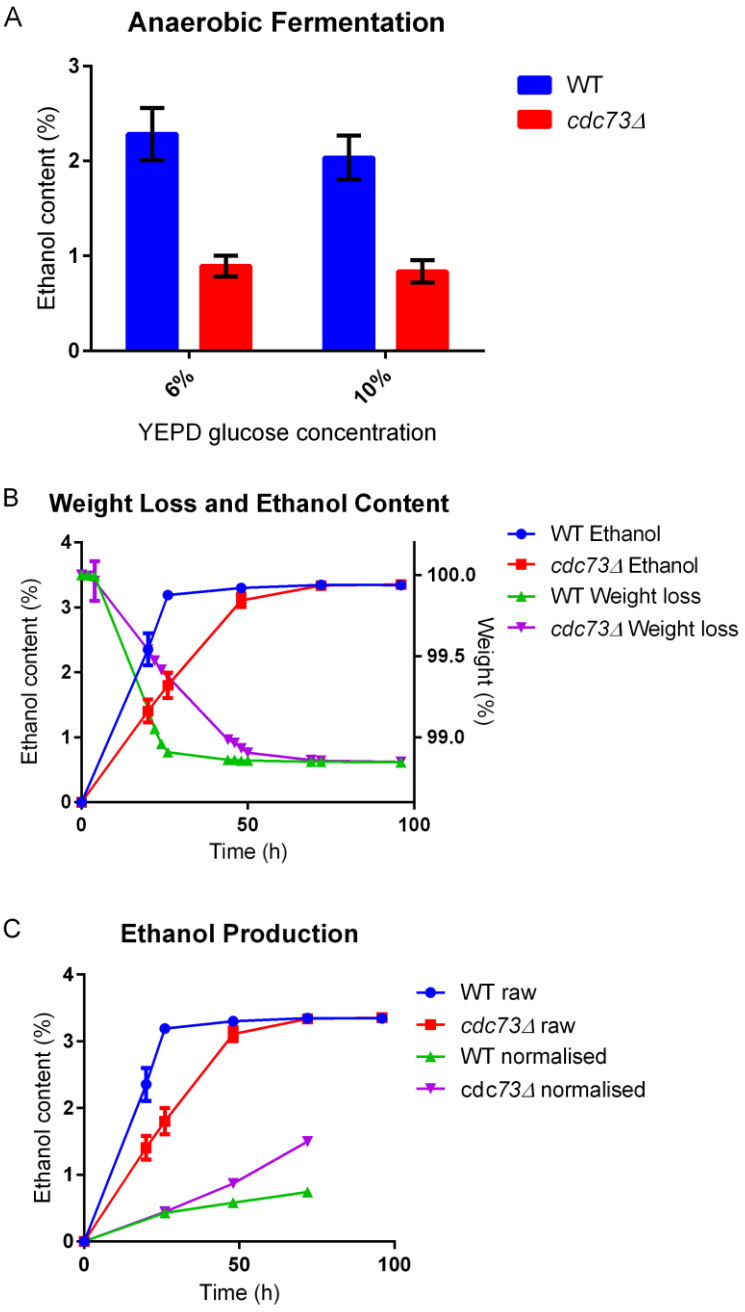


Figure 17. Ethanol production analysis of WT and *cdc73Δ* yeast. (A) Ethanol content of two media (YEPD containing 6% and 10% glucose w/v) after 5 d static anaerobic fermentation using WT and *cdc73Δ* cells. Values are means of three independent replicates +/- SEM. (B) Weight loss of fermentation vessels (right axis) and increase in medium ethanol content % ethanol v/v (left axis) over time in both WT and *cdc73Δ* cells. (C) Ethanol production over time by WT and *cdc73Δ* cells. "Raw" data relates to absolute concentration in the medium; "normalised" is after correction for the higher cell concentrations produced by the wild type.

3.10 Repeat of tests for diauxie during WT and *cdc73Δ* yeast growth

Because the above ethanol analyses were inconsistent with the original indications of ethanol-deficient growth by the *cdc73Δ* mutant, the cells were again grown on YEPD with three difference glucose concentrations, in the same manner as in *3.7 Comparison of WT and cdc73Δ yeast growth pre- and post-diauxic shift*. This time, in all three replicates the growth curves of both WT and *cdc73Δ* cells showed a second growth phase (Figure 18). The experiment was repeated again, and again a clear diauxic shift to slower respiratory growth by the *cdc73Δ* mutant was evident. Adding ethanol to the medium had no effect on the curves (data not shown). The outcomes were now reproducibly different to the original experiment (Figure 15A, B). This combined with the ethanol production data (Figure 17B) strongly implied that the original triplicate growth curves lacking a second growth phase were an anomaly.

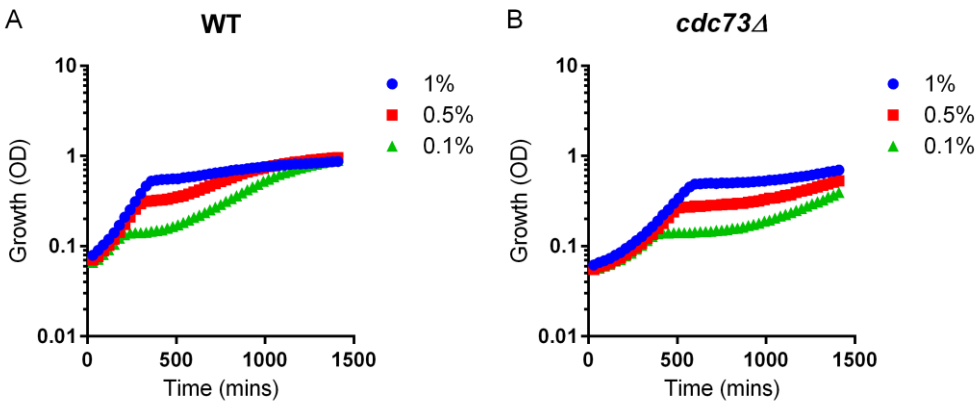


Figure 18. Repeat of diauxie growth curves of WT and *cdc73Δ* yeast. (A) WT growth curves on YEPD containing 1, 0.5 and 0.1% glucose w/v. (B) *cdc73Δ* mutant growth curves on YEPD containing 1, 0.5 and 0.1% glucose Growth curves are of single representative experiments (see Note in legend to Figure 6).

3.11 Hyper-sensitivity of the *cdc73Δ* mutant to artesunate may not be dependent on the presence of oxygen

The hypothesis of artesunate damage being mediated via ROS was revisited by culturing WT and *cdc73Δ* yeast under anaerobic conditions. As broth culturing was difficult to achieve anaerobically, these tests were performed by spotting assays on agar medium. Due to the high concentrations required and expense of artesunate, spotting assays were performed in 48-well plates rather than petri dishes. Growth in the anaerobic chamber was slowed for both strains, but the impact appeared greatest in *cdc73Δ* colonies. Despite the slowed growth of the *cdc73Δ* mutant in anaerobic conditions, it still seemed to be hyper sensitive to artesunate compared to the WT on YEPD agar medium (Figure 19). The results of this assay were often difficult to interpret as the *cdc73Δ* mutant did not show consistent behaviour. For example in Figure 19 there appears to be little difference in growth rate between WT and *cdc73Δ* colonies at 0M artesunate, but the slowed growth rate of *cdc73Δ* yeast that has been shown by growth curves (Figure 7A) was apparent in other spotting replicates. Considering all replicates of the experiment, it appears that the increased sensitivity of the *cdc73Δ* mutant is not dependant on the presence of oxygen, and as such the cause of artesunate damage may not be mediated via ROS production. However, this should ideally be verified using anaerobic growth curves.

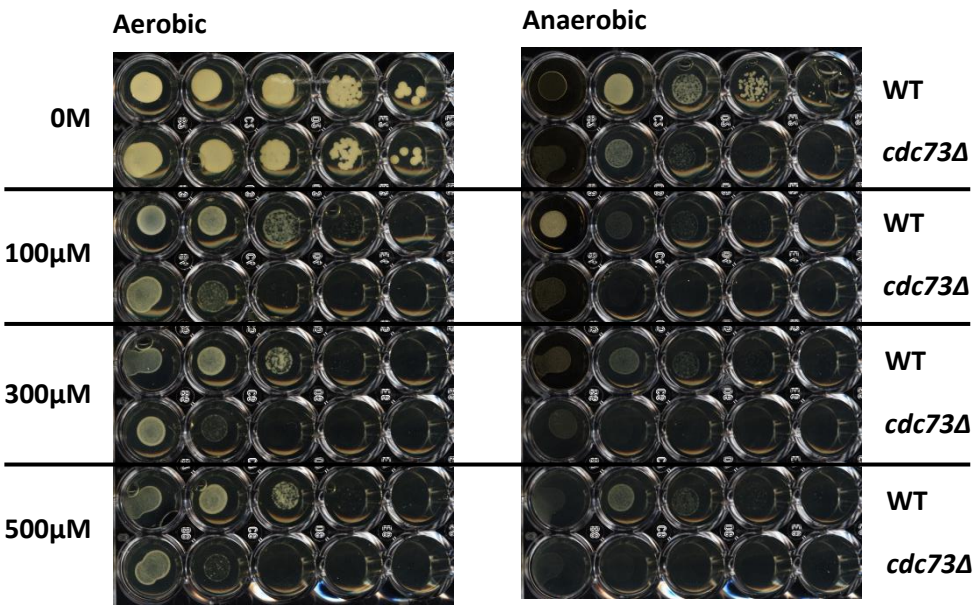


Figure 19. Spotting assay of WT and *cdc73Δ*. Scan of spotting assay of WT (upper spot) and *cdc73Δ* (lower spot) yeast colonies. Left: Aerobic, Right: Anaerobic. Top to bottom: 0M | 100µM | 300µM | 500µM artesunate. An unnoticed heat source in the anaerobic chamber resulted in several of the leftmost wells drying out and potentially also affecting growth rate of the spots contained within. These spots were ignored during analysis.

3.12 The yeast deletion mutant *adh1Δ* shows increased sensitivity to artesunate on YEPD medium

In conjunction with the artesunate sensitivity of *cdc73Δ* cells only being evident on fermentable medium, another link to the fermentation pathway here is that Cdc73p has a reported interaction with the mRNA encoding the alcohol dehydrogenase enzyme Adh1p (Dermody and Buratowski 2010). Adh1p is the primary enzyme responsible for catalysing the final stage of ethanol synthesis (Leskovac et al. 2002), and lacking *ADH1* significantly reduces the rate of ethanol production by yeast (Cordier et al. 2007). Cdc73p has a role in regulation of gene expression and it was hypothesised that the impact of Cdc73p on artesunate resistance could be mediated indirectly,

through the protein's reported interaction with *ADH1*. The original screen of mutants carried out in the Avery laboratory prior to the start of this project did not include the *adh1Δ* mutant, as this mutant failed to grow when thawed from frozen stocks. A new copy of the mutant was purchased to test the hypothesis that it may show artesunate sensitivity on fermentable medium. As hypothesised, the *adh1Δ* mutant did show artesunate sensitivity on YEPD. 50µM artesunate was sufficient to strongly inhibit mutant growth, whereas the effect on WT was negligible (Figure 20A). This level of sensitivity was greater than that shown by *cdc73Δ* cells. The increased sensitivity of the *adh1Δ* mutant was not evident on YEPG (data not shown).

3.13 Extracellular ethanol concentration does not affect sensitivity of *adh1Δ* cells to artesunate on YEPD medium

A major phenotype of the *adh1Δ* mutant is its reduced ethanol production (Cordier et al. 2007). The sensitivity of WT and *adh1Δ* cells to artesunate was measured with varying concentrations of ethanol added to the YEPD in order to establish whether a difference in the concentration of extracellular ethanol was affecting the drug sensitivity of either strain. Growth curves for WT and *adh1Δ* cells were produced using YEPD containing four different concentrations of ethanol (0, 1, 2, and 3% v/v), with and without 30µM artesunate. The ethanol concentration of YEPD in the absence or presence of artesunate had no significant effect on the doubling times of WT or *adh1Δ* cells (two way ANOVA all p values >0.05) (Figure 20B).

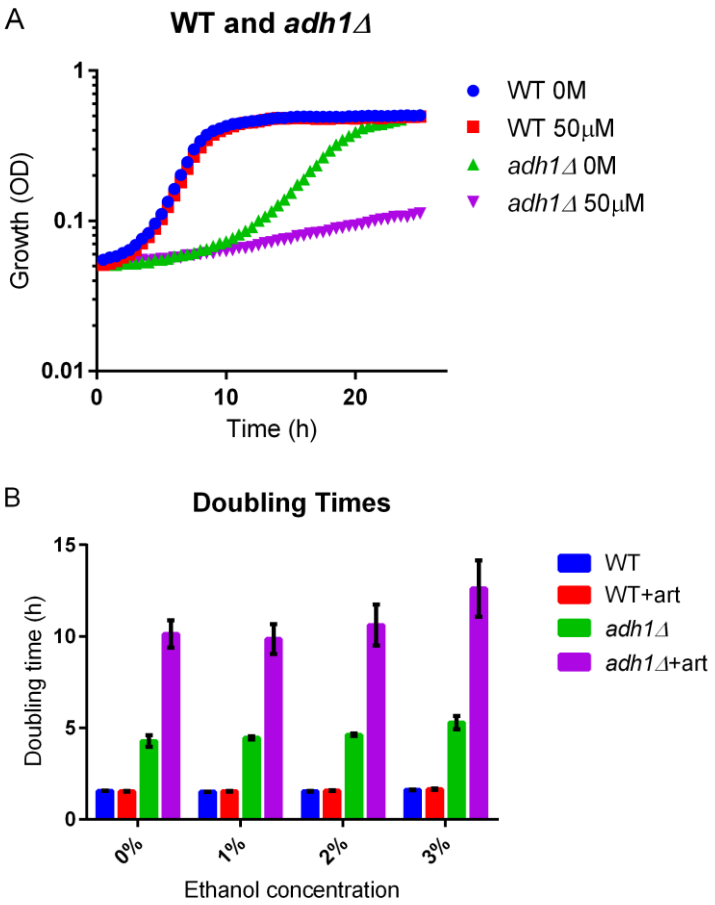


Figure 20. WT and *adh1Δ* yeast growth curves and doubling times in YEPD supplemented with ethanol. (A) Growth curves of WT and *adh1Δ* cells in YEPD in the presence and absence of 50μM artesunate. Growth curves are of representative experiments from at least three independent replicates (see Figure 6 legend). (B) Doubling times of WT and *adh1Δ* cells in YEPD with additional ethanol in the presence and absence of 30μM artesunate. Values are mean of three independent replicates +/- SEM.

3.14 Overexpression of *ADH1* in WT and *cdc73Δ* backgrounds does not improve artesunate resistance

ADH1 was overexpressed in the WT by cloning the *ADH1* sequence into pCM190 and transforming the resulting plasmid into WT yeast (WT+ *ADH1*, details in *2.7 Plasmid constructions* and Figure 4, plasmid verified by restriction digest, Figure 8B). The transformant showed no difference in growth rate or artesunate sensitivity to the untransformed WT, with both

producing very similar growth curves (Figure 21). This implies that Adh1p is not a direct target of artesunate, despite being necessary for normal levels of resistance. *ADH1* was also overexpressed in the *cdc73Δ* background to see if it could rescue its artesunate sensitivity. Again there was also no difference in sensitivity between the *cdc73Δ* mutant and a *cdc73Δ* mutant overexpressing *ADH1* (Figure 22). This suggested that an Adh1p defect is not the cause of artesunate sensitivity of the *cdc73Δ* mutant.

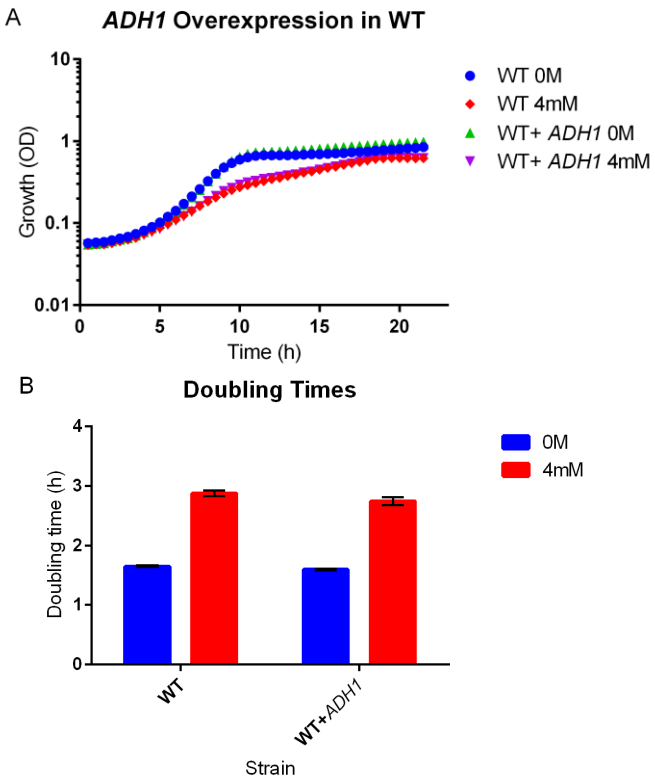


Figure 21. Growth of WT cells overexpressing *ADH1*. (A) Growth curves of WT and WT transformed with pCM190-*ADH1* (WT+ *ADH1*) in YEPD, in the presence and absence of 4mM artesunate. Growth curves are of representative experiments from at least three independent replicates (see Note in legend to Figure 6). (B) Mean doubling times of WT and WT+ *ADH1* in YEPD in the presence and absence of 0.5mM Artesunate +/- SEM.

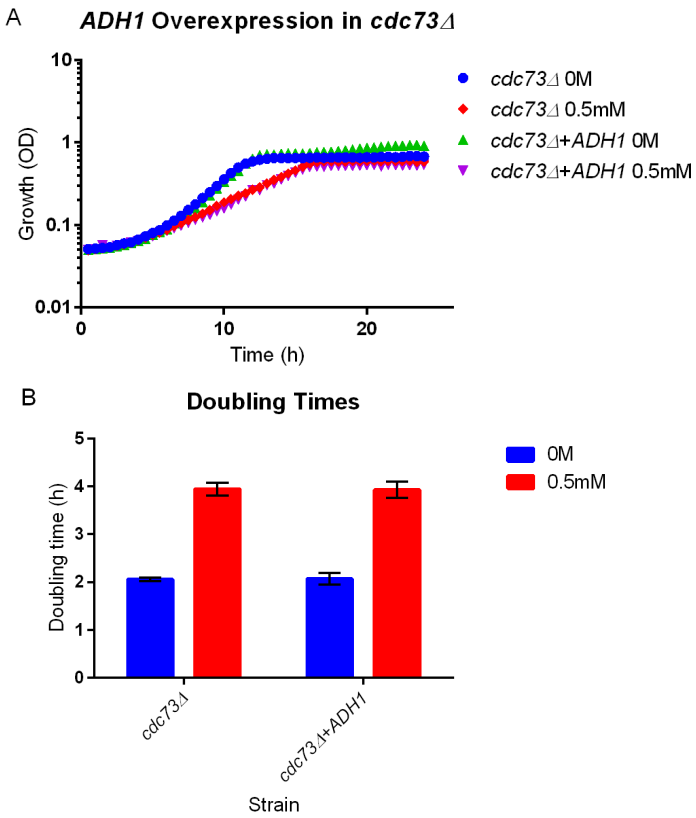


Figure 22. Growth of *cdc73Δ* cells overexpressing *ADH1*. (A) Growth curves of *cdc73Δ* and *cdc73Δ* transformed with pCM190-*ADH1* (*cdc73Δ*+ *ADH1*) in YEPD, in the presence and absence of 0.5mM artesunate. Growth curves are of representative experiments from at least three independent replicates (see Note in legend to Figure 6). (B) Mean doubling times of *cdc73Δ* and *cdc73Δ*+ *ADH1* in YEPD, in the presence and absence of 0.5mM artesunate +/- SEM.

3.15 Increased sensitivity *of adh1Δ* cells to artesunate is dependent on the presence of oxygen

A spotting assay of WT and *adh1Δ* on YEPD agar containing artesunate revealed that increased *adh1Δ* mutant sensitivity only manifests itself in an aerobic environment. Growth of *adh1Δ* colonies in anaerobic conditions were practically indistinguishable across all concentrations of artesunate used. This was also true of the WT over this 0-50µM artesunate concentration range. In the presence of oxygen, increasing inhibition was visible as the concentration of artesunate increased for both WT and mutant, but this effect was far more pronounced in *adh1Δ* colonies (Figure 23). This is evidence that increased sensitivity to artesunate in *adh1Δ* cells is dependent on the presence of oxygen and could be mediated via ROS.

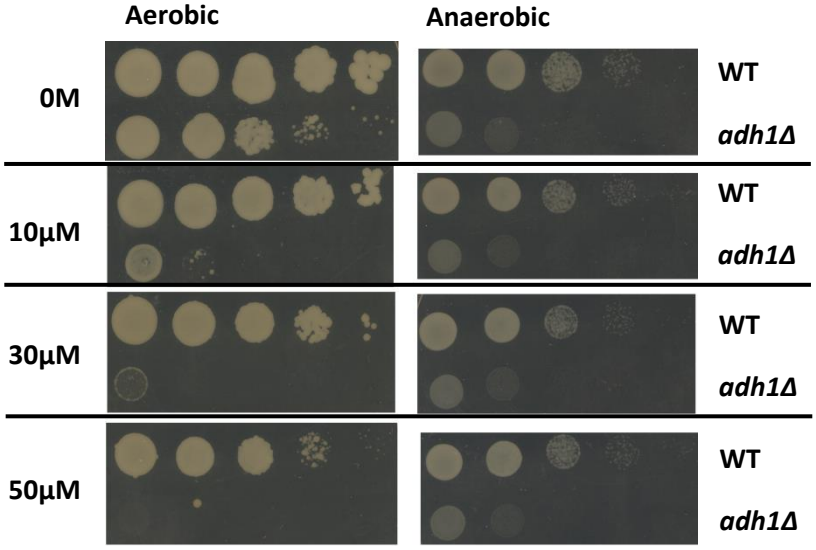


Figure 23. WT and *adh1Δ* spotting assay. Scan of spotting assay of WT (upper spot) and *adh1Δ* (lower spot) colonies. Left Aerobic, Right Anaerobic. Top to bottom: 0M | 10µM | 30µM | 50µM artesunate.

3.16 Increased sensitivity to artesunate in *adh1Δ* cells is not a consequence of a change in the activity of the glycerol production pathway

If *ADH1* is not a direct target of artesunate, then it was hypothesised that the drug may interact with pathways which show altered activity in the absence of *ADH1* activity. The glycerol production pathway is active at low levels in WT yeast grown on YEPD, and produces relatively small quantities of glycerol. It has been proposed that the pathway acts as a sink for excess NADH when an imbalance of NAD^+: NADH occurs (Bakker et al. 2006). The pathway is known to be up-regulated in *adh1Δ* cells (Cordier et al. 2007), presumably to compensate for the loss of the NADH oxidising role of Adh1p (De Smidt et al. 2008). If the glycerol production pathway is a target of artesunate, then up or down-regulating the pathway in WT yeast may be expected to modify artesunate resistance. The gene *GPD1* encodes a key enzyme in the pathway, and its deletion and overexpression have been shown to down-regulate and up-regulate glycerol production respectively (Michnick et al. 1997 and Cordier et al. 2007). The role of *GPD1* in artesunate sensitivity was investigated. Yeast lacking *GPD1* were tested for artesunate sensitivity. It was found that *gpd1Δ* yeast showed no difference in growth rate or sensitivity to artesunate relative to WT (Figure 24). The *GPD1* sequence was cloned into pCM190 in the same way as *CDC73* and *ADH1* above (details in *2.7 Plasmid constructions* and Figure 4, plasmid verified by restriction digest, Figure 8C). WT yeast transformed with the plasmid (WT+

GPD1) also showed no change in growth rate or sensitivity to artesunate relative to WT (Figure 25). From this evidence it was concluded that the *adh1Δ* mutant sensitivity to artesunate is not a result of a change in the activity of the glycerol production pathway.

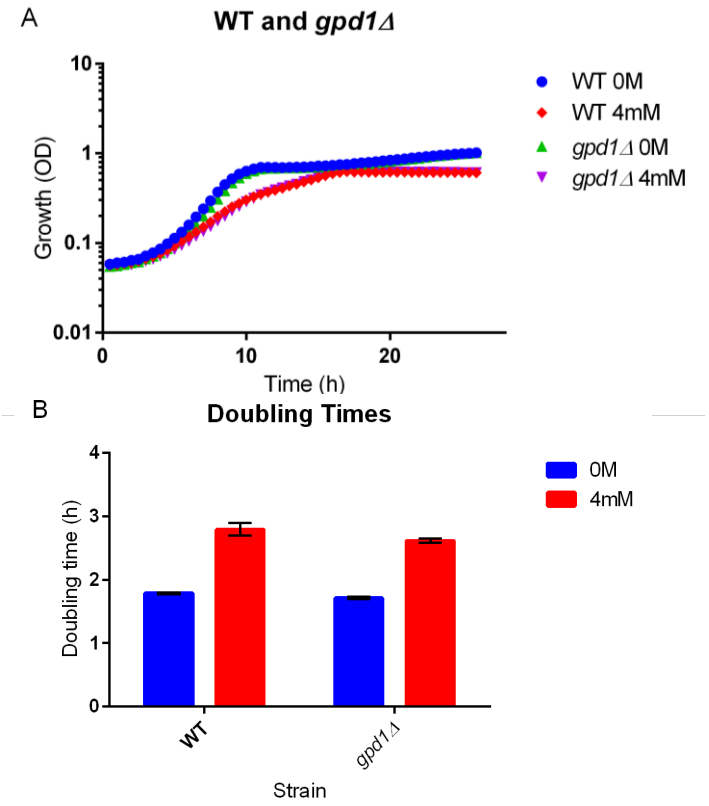


Figure 24. Growth curves of yeast with down-regulated and up-regulated glycerol production pathway. (A) Growth curves of WT and *gpd1Δ* cells in YEPD in the presence and absence of 4mM artesunate. Growth curves are of representative experiments from at least three independent replicates (see Note in legend to Figure 6). (B) Mean doubling times of WT and *gpd1Δ* cells in YEPD in the presence and absence of 4mM artesunate +/- SEM.

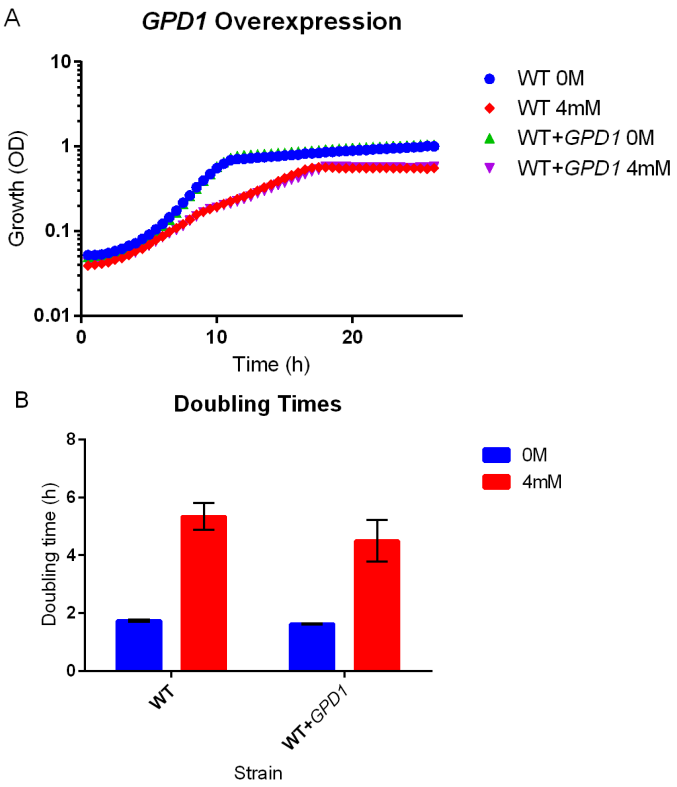


Figure 25. Growth curves of yeast with down-regulated and up-regulated glycerol production pathway. (A) Growth curves of WT and WT transformed with *GPD1* overexpression plasmid pCM190-*GPD1* (WT+ *GPD1*) in YEPD, in the presence and absence of 4mM artesunate. Growth curves are of representative experiments from at least three independent replicates (see Note in legend to Figure 6). (B) Mean doubling times of WT and WT+ *GPD1* in YEPD, in the presence and absence of 4mM artesunate +/- SEM.

4. Discussion

The aim of this project was to use the budding yeast *Saccharomyces cerevisiae* in order to investigate the mode of action of the antimalarial drug artesunate. Artesunate has been shown to cause growth inhibition in yeast so continuing from previous work in the Avery laboratory, deletion mutants from the yeast deletion collection were screened for changes in sensitivity to identify potential targets of the drug. With this information on drug sensitive mutants, particular leads could be pursued to gain more insight. The principal finding of this research is that the proteins Cdc73p and Adh1p are required for resistance of yeast to artesunate, in a manner that depends on fermentative growth.

4.1 Cdc73p and the Paf1p complex

Cdc73p functions as part of the Paf1p complex, which among other functions is involved in modulation of the activity of RNA polymerase II (Mueller and Jaehning 2002). The increased sensitivity of *cdc73Δ* cells to artesunate could indicate that artesunate may interfere with gene transcription. Deletions of the three available Paf1p complex genes all resulted in some form of decreased growth rate of the yeast (Figure 7A, 10); however deletion of *CDC73* resulted in the greatest increase in doubling time and was the only mutant to show increased sensitivity to artesunate. This is evidence that artesunate hyper sensitivity may be specifically related to Cdc73p activity, and not the whole Paf1p complex. Furthermore the fact that

the *cdc73Δ* mutant experiences the greatest increase in doubling time even in the absence of artesunate suggests that Cdc73p may play the most important role within the protein complex for normal fermentative yeast growth.

4.2 Superoxide levels in WT and *cdc73Δ* strains of yeast

The DHE assay showed that the level of superoxide in *cdc73Δ* cells is far higher than in WT yeast cells. This could potentially be due to excessive leakage of superoxide from the mitochondria, as the mutant has been shown to have abnormal mitochondrial morphology and experiences a higher frequency of spontaneous mitochondrial genome loss (Dimmer et al. 2002 and Hess et al. 2009). The levels of superoxide however were not increased by the presence of artesunate in either the WT or the mutant. If artesunate is damaging WT and *cdc73Δ* cells by production of free radicals as in some predicted models of artesunate action (e.g., Wang et al. 2010), then the DHE assay results imply that the drug does not generate superoxide. In contrast, previous research has demonstrated that superoxide scavengers will reduce cytotoxicity of dihydroartemisinin to leukaemia cells (Zhang et al. 2010). It is possible that superoxide scavenging is more efficient in yeast or that ROS generation may differ for the different artemisinin-related drugs. Either way, this project found no evidence that artesunate action in yeast involved elevated superoxide levels.

4.3 Ethanol production by *cdc73Δ* cells

The progressive loss of medium weight and increase in ethanol accumulation that occurred during yeast growth in this study appeared balanced. Both the WT and *cdc73Δ* strains appeared to halt ethanol production when the ethanol content of the medium reached ~3.3%. Cell counts were taken at three time points during the fermentation, which allowed ethanol production of the two strains to be normalised. This indicated that ethanol production by *cdc73Δ* cells was actually higher than the WT at later stages in growth. This may be a result of the final two cell counts being taken as ethanol concentration reached a plateau, during which the ethanol content changed very little whereas the proportion of viable cells in both WT and *cdc73Δ* cultures began to decrease. If a constant absolute concentration is being divided between fewer and fewer cells over time, once normalised it would appear that the culture is still producing ethanol. If this experiment were to be repeated, as the timing of the growth curve is now known it would be possible to take cell counts during the exponential phase of growth. This would help produce a more accurate representation of ethanol production. Although the data gathered is insufficient to accurately comment on the relative rates of ethanol production between the WT and the *cdc73Δ* mutant, it is possible to conclude that *cdc73Δ* cells are not deficient for ethanol production. During the fermentations, an additional phenotype of *cdc73Δ* yeast was observed. Samples of medium from the first 12 fermentation vessels were frozen after extraction so that all media

samples could be analysed for ethanol content at the same time. When thawing the frozen samples, sediment had precipitated out of the *cdc73Δ* culture medium, but not for the WT. The sediment could be completely re-dissolved by vortexing. This indicates that *cdc73Δ* cells are producing a metabolite that the WT is not. There was insufficient time in the project to pursue this observation further, but it would be of interest to characterise the sediment composition as it could shed further light on Cdc73p-specific artesunate action.

4.4 Diauxie in WT and *cdc73Δ* yeast cultures

Due to the mounting evidence contradicting the initial indication that the *cdc73Δ* mutant was deficient for post diauxic growth, the experiment was repeated several times including with the addition of ethanol. Reproducibly, the *cdc73Δ* mutant did now produce a second growth phase, regardless of the presence of ethanol in the medium. Why this difference compared with the initial experiments? As was mentioned earlier, the mutant has been shown to prone to mitochondrial irregularities (Dimmer et al. 2002 and Hess et al. 2009). As yeast lacking functional mitochondria does not show diauxie when grown on fermentable media, it is possible that the original growth curves for the *cdc73Δ* mutant may have been produced with clones that had suffered a spontaneous event causing mitochondrial dysfunction. The original result was reproducible at the time across cultures generated from three independent *cdc73Δ* colonies. However, those colonies had been generated by previous restreaking from a single colony of an earlier plate, so were

historically linked. An early spontaneous mitochondrial defect could have been inherited in offspring right up to the experiment. A fresh culture generated from frozen stocks was used for the later experiment. The original plates were unfortunately not retained to assay for mitochondrial activity.

4.5 The role of oxygen in artesunate hypersensitivity of the *cdc73Δ* mutant

The slow growth rate of *cdc73Δ* cells under anaerobic conditions made the results of spotting assays difficult to interpret, and far more reliable data could be obtained by housing a plate reader in an anaerobic chamber to produce growth curves. The possibility that the increased sensitivity of the *cdc73Δ* mutant to artesunate still manifests itself when grown in anaerobic conditions is further evidence that the hyper-sensitivity of this mutant may be by a separate mechanism to ROS damage to the mitochondria characterised elsewhere (Wang et al. 2010). In addition to other research implicating calcium channels as a target of the drug, artesunate has also been shown to be active against human cancer cells (Holien et al. 2013). The human homologue of *CDC73* encodes parafibromin -a tumour suppressor- and mutations in human *CDC73* have been linked to cancers (Howell et al. 2003). Overexpression of the human protein blocks cell proliferation and expression of cyclin D1, a key cell cycle regulator (Woodard et al. 2005). The action of artesunate against *cdc73Δ* yeast could well be related to the specificity of its action against human tumour cells and this aspect warrants further research.

4.6 Inconsistent behaviour of the *cdc73Δ* mutant

Throughout the project, the sensitivity of the *cdc73Δ* mutant was found to vary. The initial growth curves produced showed strong growth inhibition at 1mM artesunate; however, in certain later tests the mutant appeared only marginally more sensitive than the WT. Several approaches were tested to try to resolve the issue, for example fresh drug stocks or a fresh aliquot of the strains being thawed from -80°C stocks, but the inconsistent sensitivity still remained. The variability may possibly be explained by the aforementioned mitochondrial differences in the mutant (Dimmer et al. 2002 and Hess et al. 2009). As was shown in Figure 16, petite mutants of both WT and *cdc73Δ* strains are sensitised to artesunate implying that functional mitochondria are necessary for normal resistance on YEPD. If populations of *cdc73Δ* mutants are becoming spontaneously petite, this could be one factor contributing to their artesunate sensitivity, and variation therein. In that case, lacking *CDC73* may not be the direct cause of hyper sensitivity to artesunate; rather it is a result of any related damage to the mutant's mitochondria. Another element of variability within *cdc73Δ* cells was apparent when performing spotting assays. In some of the *cdc73Δ* cultures, small populations of colonies within a spot appeared to be growing faster even than the WT. Similar cell to cell (colony to colony) heterogeneity has been well documented for other phenotypes (Avery 2006).

4.7 Hyper sensitivity of *cdc73Δ* cells to artesunate is unrelated to a lack of Adh1p

The data obtained showing that the *cdc73Δ* mutant was sensitive to artesunate only when growing in fermentable media, along with a known interaction between Cdc73p and *ADH1* mRNA (Dermody and Buratowski 2010) and the role of Cdc73p in regulating gene expression, lead to the hypothesis that a lack of Adh1p activity may be the cause of artesunate hyper-sensitivity in *cdc73Δ* cells. However, the following evidence argued against this: artesunate sensitivity in an *adh1Δ* mutant was markedly more severe than in a *cdc73Δ* mutant; overexpressing *ADH1* in the *cdc73Δ* background did not rescue its sensitivity; and *adh1Δ* mutant sensitivity is strongly attenuated by the absence of oxygen whereas *cdc73Δ* mutant sensitivity was not. From these findings it was concluded that that the sensitivity of the *cdc73Δ* cells is not result of an absence of Adh1p activity.

4.8 Hypersensitivity to artesunate of the *adh1Δ* mutant

Adh1p is the primary alcohol dehydrogenase responsible for the conversion of acetaldehyde to ethanol in the final stage of fermentation (De Smidt et al. 2011). In the spotting assay, the sensitivity of WT and *adh1Δ* cells to artesunate only manifested itself in the presence of oxygen, which is consistent with existing research suggesting that degradation of artemisinins leads to the production of ROS which in turn damages the cells (Zhang and Gerhard 2008). Although growth inhibition by artesunate from 10 to 50µM in

aerobic conditions is present in both WT and *adh1Δ*, the fact that the sensitivity of *adh1Δ* is far more pronounced implies that a pathway that is inactive (or active at low levels) in the WT but active in *adh1Δ* cells is causing the activation of artesunate. This potentially could be a pathway to compensate for a shortfall in NAD^+ regeneration. As altering the activity of the glycerol production pathway had no effect on artesunate sensitivity in the WT, other pathways that regenerate NAD^+ could be considered. Similar approaches to those taken here initially to investigate the hyper-sensitivity of the *cdc73Δ* mutant could be pursued with the *adh1Δ* mutant. For example inappropriate NADH dehydrogenase activity or of components of the aerobic respiration pathway may be a feature of *adh1Δ* cells grown on YEPD. Petite variants of *adh1Δ* cells could be tested to see if this influences drug sensitivity. The *adh1Δ* mutant is known to have increased sensitivity to oxidative stress (Begley et al. 2004). In addition, this mutant has an incomplete fermentation pathway, while artesunate sensitivity (of wild type cells) is greatly accentuated in non-fermentable media. These indirect relationships could explain the basis of the mutant's sensitivity to this antimalarial drug rather than a specific target that is closer to Adh1p activity.

4.9 Genotoxicity assays

The first attempt at an artesunate genotoxicity test using a Rad54p-GFP fusion failed to produce any quantifiable GFP, even when exposed to positive-control genotoxins. This method that integrated the tag into the yeast genome was only analysed using fluorescence microscopy. According to the

original *RAD54*-GFP work, the levels of GFP produced are often not sufficient to be visualised this way (Cahill et al. 2004). It would be advisable to repeat the assay again using a fluorescence microplate reader or flow cytometer for analysis. In the second approach to this assay, the *RAD54*-GFP fusion was expressed from a plasmid rather than integrating the tag into the genome. Analysis with flow cytometry indicated that artesunate had no effect on fluorescence of either untransformed WT cells or cells transformed with the pRS315-*RAD54*-GFP plasmid. Although not conclusive, the results suggest that artesunate does not cause significant DNA damage. These results are at odds with unpublished data from the Avery laboratory showing *OGG1* deletion increases yeast sensitivity to artesunate. Cells lacking this DNA repair protein being sensitised to artesunate indicates that the drug may be genotoxic. This along with other research demonstrating that artesunate can cause DNA double strand breaks in cancer cells (Berdelle et al. 2011) suggests that the genotoxicity assay could have produced a false negative, or that the DNA damage produced by artesunate is not of a nature that activates *RAD54*.

4.10 Conclusions

The findings of this project indicate that both Cdc73p and Adh1p activity are necessary for normal artesunate resistance in yeast, but they themselves are not direct targets of the drug.

The inconsistent behaviour of the *cdc73Δ* mutant, along with the protein's large number of functions and interactions with other genes (over 600 are listed on the *Saccharomyces* Genome Database) ultimately made it

difficult to establish exactly why the mutant was sensitive to artesunate within the time frame of the project. However, the findings presented could be consistent with a drug target that is not dependent on the activity of mitochondria. Sensitivity caused in cells lacking *CDC73* may well provide insight as to why artesunate is specifically active against mammalian cancer cells, and it would be of interest to measure the effect of artemisinins on mammal cell lines with defective *CDC73*, but the mechanism by which artesunate causes damage to yeast cells lacking Cdc73p activity is less clear. If the hyper sensitivity of *cdc73Δ* cells is in fact not dependent on the presence of oxygen, this would suggest that the target of artesunate is not in the mitochondria, and unrelated to a mechanism characterised by ROS production. Since *CDC73* is a cell division cycle gene, it is possible that yeast cells' sensitivity to artesunate varies during different stages of their division cycle. There is also evidence discussed earlier that artesunate may interfere with the cell cycle during mitotic spindle formation (Steinbrück et al. 2011). It may be useful to pursue this line of research by testing other *S. cerevisiae* deletion mutants that are known to have irregularities within their cell cycle for artesunate sensitivity. If increased artesunate sensitivity of *cdc73Δ* cells is dependent on the presence of oxygen, this may mean that the drug may be damaging the cells in a way similar to the mechanisms already demonstrated in yeast grown on respiratory medium (Wang et al 2010). It would be useful to produce anaerobic growth curves of *cdc73Δ* yeast in the presence of artesunate to further elucidate this. A BLAST analysis of the *S. cerevisiae* *CDC73* sequence reveals that there are several uncharacterised or

hypothetical proteins across several species of *Plasmodium* that show sequence similarity to *CDC73*. The conserved nature of *CDC73* suggests that the findings presented here may be relevant to *Plasmodium* models. However, the fact that the *cdc73Δ* mutant's increased sensitivity to artesunate does not manifest itself on both fermentable and non-fermentable carbon sources suggests this may be a phenotype specific to yeast. As it only manifests itself on fermentable media, this indicates that the drug mechanism of action is possibly related to the fermentation pathway. *Plasmodium* does not produce ethanol, so if fermentation is necessary for the increased sensitivity of *cdc73Δ* cells then the phenotype observed in mutant *S. cerevisiae* may not be present in *Plasmodium*. If it is possible to achieve a *Plasmodium* mutant lacking its equivalent of *CDC73*, it would be useful to test it for changes in its sensitivity to artemisinins.

Data obtained from the *adh1Δ* mutant suggest that changes in yeast metabolism (e.g. partial activation of elements of the electron transport chain) may be the cause of its hyper sensitivity to artesunate on YEPD. If this is the case, the mechanism by which artesunate inhibits growth of *adh1Δ* cells on fermentable medium could be similar to the hypothesised action of artemisinins in yeast grown on non-fermentable carbon sources, involving drug activation by mitochondrial activity, leading to free radical generation and subsequent cell damage. This could be established by further researching the effect a lack of Adh1p activity has on *S. cerevisiae*, and what changes may occur to its metabolism. BLAST analysis of the *S. cerevisiae* sequence of *ADH1*

showed low sequence similarity to the *P. vivax* gene *VIR6*. *Plasmodium* does not appear to have orthologs of alcohol dehydrogenase, so research done using *adh1Δ* yeast may only indicate general details of the mode of action of artesunate in *Plasmodium* rather than specific mechanisms.

5. References

Achan J, et al. (2009) Effectiveness of quinine versus artemether-lumefantrine for treating uncomplicated falciparum malaria in Ugandan children: randomised trial. British Medical Journal 339:b2763

Achan J, et al. (2011) Quinine, an old anti-malarial drug in a modern world: role in the treatment of malaria. Malaria Journal 10:144

Amberg DC, Burke D, Strathern JN (2005) Methods in Yeast Genetics: A Cold Spring Harbor Laboratory Course Manual. Cold Spring Harbor Laboratory Press, Cold Spring Harbor, New York.

Antoine T, Fisher N, Amewu R, O'Neill PM, Ward SA, Biagini GA (2014) Rapid kill of malaria parasites by artemisinin and semi-synthetic endoperoxides involves ROS-dependent depolarization of the membrane potential. Journal of Antimicrobial Chemotherapy 69:1005-1016

Avery SV (2006) Microbial cell individuality and the underlying sources of heterogeneity. Nature Reviews Microbiology 4:577-587

Avery SV (2011) Molecular targets of oxidative stress. The Biochemical Journal 434:201-210

Bakker BM, Overkamp KM, van Maris AJA, Kötter P, Luttik MAH, van Dijken JP, Pronk JT (2006) Stoichiometry and compartmentation of NADH metabolism in *Saccharomyces cerevisiae*. FEMS Microbiology Reviews 25:15-37

Bartoloni A, Zammarchi L (2012) Clinical Aspects of Uncomplicated and Severe Malaria. Mediterranean Journal of Hematology and Infectious Diseases 4:e2012026

Bateman DN, Dyson EH (1986) Quinine toxicity. Adverse Drug Reactions and Acute Poisoning Review 5:215-253

Begley TJ, Rosenbach AS, Ideker T, Samson LD (2004) Hot spots for modulating toxicity identified by genomic phenotyping and localization mapping. Molecular Cell 16:117-125

Berdelle N, Nikolova T, Quiros S, Efferth T, Kaina B (2011) Artesunate induces oxidative DNA damage, sustained DNA double-strand breaks, and the ATM/ATR damage response in cancer cells. Molecular Cancer Therapeutics 10:2224-2233

Bolotin-Fukuhara M, Dumas B, Gaillardin C (2010) Yeasts as a model for human diseases. FEMS Yeast Research 10:959–960

Botstein D, Chervitz SA, Cherry JM (1997) Yeast as a Model Organism. Science 277:1259-1260

Cahill PA, Knight AW, Billinton N, Barker MG, Walsh L, Keenan PO, Williams CV, Tweats DJ, Walmsley RM (2004) The GreenScreen® genotoxicity assay: a screening validation programme. Mutagenesis 19:105-119

Centers for Disease Control and Prevention (2012) The History of Malaria, an Ancient Disease. http://www.cdc.gov/malaria/about/history/. Accessed 23 August 2014

Chaves LF, Koenraadt CJ (2010) Climate change and highland malaria: fresh air for a hot debate. The Quarterly Review of Biology 85:27-55

Chinappi M, Via A, Marcatili P, Tramontano A (2010) On the Mechanism of Chloroquine Resistance in *Plasmodium falciparum*. PLoS One 5:e14064

Cordier H, Mendes F, Vasconcelos I, François JM (2007) A metabolic and genomic study of engineered *Saccharomyces cerevisiae* strains for high glycerol production. Metabolic Engineering 9:364-378

Cox FEG (2010) History of the discovery of the malaria parasites and their vectors. Parasites and Vectors 3:5

De Smidt O, du Preez JC, Albertyn J (2008) The alcohol dehydrogenases of *Saccharomyces cerevisiae*: a comprehensive review. FEMS Yeast Research 8:967-978

De Smidt O, du Preez JC, Albertyn J (2011) Molecular and physiological aspects of alcohol dehydrogenases in the ethanol metabolism of *Saccharomyces cerevisiae*. FEMS Yeast Research 12:33-47

Dermody JL, Buratowski S (2010) Leo1 Subunit of the Yeast Paf1 Complex Binds RNA and Contributes to Complex Recruitment. The Journal of Biological Chemistry 285:33671-33679

Dimmer KS, Fritz S, Fuchs F, Messerschmitt M, Weinbach N, Neupert W, Westermann B (2002) Genetic basis of mitochondrial function and morphology in *Saccharomyces cerevisiae*. Molecular Biology of the Cell 14:847-853

Faurant C (2011) From bark to weed: The history of artemisinin. Parasite 18:215-218

Ferri FF (2009) Ferri's Color Atlas and Text of Clinical Medicine. Saunders Elsevier, Philadelphia PA

Galdieri L, Mehrotra S, Yu S, Vancura A (2010) Transcriptional regulation in yeast during diauxic shift and stationary phase. OMICS: A Journal of Integrative Biology 14:629-638

Garí E, Piedrafita L, Aldea M, Herrero E (1997) A Set of Vectors with a Tetracycline-Regulatable Promoter System for Modulated Gene Expression in *Saccharomyces cerevisiae*. Yeast 13:837-848

Goldring ES, Grossman LI, Marmur J (1971) Petite Mutation in Yeast. Journal of Bacteriology 107:377-381

Hempelmann E (2007) Hemozoin Biocrystallization in Plasmodium falciparum and the antimalarial activity of crystallization inhibitors. Parasitology Research 100:761-676

Hess DC, et al. (2009) Computationally driven, quantitative experiments discover genes required for mitochondrial biogenesis. PLoS Genetics 5:e1000407

Hohmann S (1991) Characterization of *PDC6*, a third structural gene for pyruvate decarboxylase in *Saccharomyces cerevisiae*. Journal of Bacteriology 173:7963-7969

Holien T, Olsen OE, Misund K, Hella H, Waage A, Rø TB, Sundan A (2013) Lymphoma and myeloma cells are highly sensitive to growth arrest and apoptosis induced by artesunate. European Journal of Haematology 91:339-346

Hommel M (2008) The future of artemisinins: natural, synthetic or recombinant? Journal of Biology 7:38

Howell VM, et al. (2003) *HRPT2* mutations are associated with malignancy in sporadic parathyroid tumours. Journal of Medical Genetics 40:657-663

Hsu E (2006) Reflections on the 'discovery' of the antimalarial qinghao. British Journal of Clinical Pharmacology 61:666-670

Islahudin F, Khozoie C, Bates S, Ting K, Pleass RJ, Avery SV (2013) Cell Wall Perturbation Sensitizes Fungi to the Antimalarial Drug Chloroquine. Antimicrobial Agents and Chemotherapy 57:3889-96

Islahudin F, Pleass RJ, Avery SV, Ting K (2012). Quinine interactions with tryptophan and tyrosine in malaria patients, and implications for quinine responses in the clinical setting. Journal of Antimicrobial Chemotherapy. 67:2501-2505

Islahudin F, Tindall SM, Mellor IR, Swift K, Christensen HEM, Fone KCF, Pleass RJ, Ting K, Avery SV (2014) The antimalarial drug quinine interferes with serotonin biosynthesis and action. Scientific Reports 4:3618

Jorgensen P, Nishikawa J L, Breitkreutz B, Tyers M (2002) Systematic Identification of Pathways That Couple Cell Growth and Division in Yeast. Science 297:395-400

Kellermann E, Seeboth PG, Hollenberg CP (1986) Analysis of the primary structure and promoter function of a pyruvate decarboxylase gene (*PDC1*) from *Saccharomyces cerevisiae*. Nucleic Acids Research 14:8963-8977

Khozoie C, Pleass RJ, Avery SV (2009) The antimalarial drug quinine disrupts Tat2p-mediated tryptophan transport and causes tryptophan starvation. The Journal of Biological Chemistry 284:17968-17974

Krishna S, Pulcini S, Moore CM, Teo BH, Staines HM (2014) Pumped up: reflections on PfATP6 as the target for artemisinins. Trends in Pharmacological Sciences 35:4-11

Leskovac V, Trivic S, Pericin D (2002) The three zinc-containing alcohol dehydrogenases from baker's yeast, *Saccharomyces cerevisiae*. FEMS Yeast Research 2:481-494

Li W, Mo W, Shen D, Sun L, Wang J, Lu S, Gitschier JM, Zhou B (2005) Yeast Model Uncovers Dual Roles of Mitochondria in the Action of Artemisinin. PLoS Genetics 1:e36

Li W, Sun L, Liang Q, Wang J, Mo W, Zhou B (2006) Yeast AMID Homologue Ndi1p Displays Respiration-restricted Apoptotic Activity and Is Involved in Chronological Aging. Molecular Biology of the Cell 17:1802-1811

Longtine MS, McKenzie A, Demarini DJ, Shah NG, Wach A, Brachat A, Philippsen P, Pringle JR (1998) Additional Modules for Versatile and Economical PCR-based Gene Deletion and Modification in *Saccharomyces cerevisiae*. Yeast 14:953-961

Meshnick SR, Taylor TE, Kamchonwongpaisan S (1996) Artemisinin and the Antimalarial Endoperoxides: from Herbal Remedy to Targeted Chemotherapy. Microbiology and Molecular Biology Reviews 60:301-315

Michnick S, Roustan JL, Remize F, Barre P, Dequin S (1997) Modulation of glycerol and ethanol yields during alcoholic fermentation in *Saccharomyces cerevisiae* strains overexpressed or disrupted for *GPD1* encoding glycerol 3-phosphate dehydrogenase. Yeast 13:783-93

Miotto O, et al. (2013) Multiple populations of artemisinin-resistant *Plasmodium falciparum* in Cambodia. Nature Genetics 45:648-655

Moore CM, Hoey EM, Trudgett A, Timson DJ (2011) Artemisinins act through at least two targets in a yeast model. FEMS Yeast Research 11:233-237

Mueller CL, Jaehning JA (2002) Ctr9, Rtf1, and Leo1 Are Components of the Paf1/RNA Polymerase II Complex. Molecular and Cell Biology 22:1971-1980

Prelich G (2012) Gene overexpression: uses, mechanisms, and interpretation. Genetics 190:841-854

Santangelo GM (2006) Glucose Signaling in *Saccharomyces cerevisiae*. Microbiology and Molecular Biology Reviews 70:253-282

Scherens B, Goffeau A (2004) The uses of genome-wide yeast mutant collections. Genome Biology 5:229

Schlagenhauf P, Adamcova M, Regep L, Schaerer MT, Rhein HG (2010) The position of mefloquine as a 21st century malaria chemoprophylaxis. Malaria Journal 2010 9:357

Seeboth PG, Bohnsack K, Hollenberg CP (1990) *pdc1*(0) mutants of *Saccharomyces cerevisiae* give evidence for an additional structural PDC gene: cloning of *PDC5*, a gene homologous to *PDC1*. Journal of Bacteriology 172:678-685

Singh KK, Sigala B, Sikder HA, Schwimmer C (2001) Inactivation of Saccharomyces cerevisiae OGG1 DNA repair gene leads to an increased frequency of mitochondrial mutants. Nucleic Acids Research 29:1381-1388

Singh KK, Singh S (2014) A Brief History of Quinoline as Antimalarial Agents. International Journal of Pharmaceutical Sciences Review and Research 25:295-302

Smith AM, et al. (2010) A survey of yeast genomic assays for drug and target discovery. Pharmacology and Therapeutics 127:156-164

Sopko R, et al. (2006) Mapping Pathways and Phenotypes by Systematic Gene Overexpression. Molecular Cell 21:319-330

Steinbrück L, Pereira G, Efferth T (2011) Effects of Artesunate on Cytokinesis and G_2/M Cell Cycle Progression of Tumour Cells and Budding Yeast. Cancer Genomics and Proteomics 7:337-346

Tomson BN, Arndt KM (2013) The many roles of the conserved eukaryotic Paf1 complex in regulating transcription, histone modifications, and disease states. Biochimica et Biophysica Acta 1829:166-126

Tu Y (2011) The discovery of artemisinin (qinghaosu) and gifts from Chinese medicine. Nature Medicine 17:1217-1220

Wang J, Huang L, Li J, Fan Q, Long Y, Li Y, Zhou B (2010) Artemisinin Directly Targets Malarial Mitochondria through Its Specific Mitochondrial Activation. PLoS One 5:e9582

Wang J, Zhou B (2010) Effect of mitochondrial electron transport inhibitors on the metabolic rate of artemisinin. Journal of Tsinghua University 50:944-946

Winzeler EA, et al. (1999) Functional characterization of the S. cerevisiae genome by gene deletion and parallel analysis. Science 285:901-906

Wongsrichanalai C, Pickard AL, Wernsdorfer WH, Meshnick SR (2002) Epidemiology of drug-resistant malaria. The Lancet Infectious Diseases 2:209-218

Woodard GE, Lin L, Zhang JH, Agarwal SK, Marx SJ, Simonds WF (2005) Parafibromin, product of the hyperparathyroidism-jaw tumor syndrome gene HRPT2, regulates cyclin D1/PRAD1 expression. Oncogene 10:1272-1276

World Health Organisation (2014) Malaria. http://www.who.int/mediacentre/factsheets/fs094/en/. Accessed 23 August 2014

Wuchty S, Barabási A, Ferdig MT (2006) Stable evolutionary signal in a Yeast protein interaction network. BioMed Central Evolutionary Biology 6:8

Zhang S, Chen H, Gerhard GS (2010) Heme synthesis increases artemisinin-induced radical formation and cytotoxicity that can be suppressed by superoxide scavengers. Chemico-Biological Interactions 1:30-35

Zhang S, Gerhard GS (2008) Heme activates artemisinin more efficiently than hemin, inorganic iron, or hemoglobin. Bioorganic and Medicinal Chemistry 16:7853-7861

6. Appendix

Table 4. Functions of corresponding genes from original 21 deletion mutants tested for artesunate sensitivity. Descriptions taken from the Saccharomyces Genome Database (www.yeastgenome.org).

Gene	Function
CDC73	Component of the Paf1p complex; binds to and modulates the activity of RNA polymerases I and II; required for expression of certain genes, modification of some histones, and telomere maintenance; involved in transcription elongation.
EST1	TLC1 RNA-associated factor involved in telomere length regulation; recruitment subunit of telomerase; has G-quadruplex promoting activity required for telomere elongation; possible role in activating telomere-bound Est2p-TLC1-RNA.
EXO1	5'-3' exonuclease and flap-endonuclease; involved in recombination, double-strand break repair, MMS2 error-free branch of the post replication (PRR) pathway and DNA mismatch repair; role in telomere maintenance.
MET18	Component of cytosolic iron-sulphur protein assembly (CIA) machinery; acts at a late step of Fe-S cluster assembly; forms the CIA targeting complex with Cia1p and Cia2p that directs Fe-S cluster incorporation into a subset of proteins involved in methionine biosynthesis, DNA replication and repair, transcription, and telomere maintenance.
MLH1	Protein required for mismatch repair in mitosis and meiosis; also required for crossing over during meiosis; forms a complex with Pms1p and Msh2p-Msh3p during mismatch repair.
MLH2	Protein involved in mismatch repair and meiotic recombination.
MLH3	Protein involved in DNA mismatch repair and meiotic recombination; involved in crossing-over during meiotic recombination; forms a complex with Mlh1p.
MSH1	DNA-binding protein of the mitochondria; involved in repair of mitochondrial DNA; has ATPase activity and binds to DNA mismatches.
MSH2	Protein that binds to DNA mismatches; forms heterodimers with Msh3p and Msh6p that bind to DNA mismatches to initiate the mismatch repair process; contains a Walker ATP-binding motif required for repair activity and involved in interstrand cross-link repair; Msh2p-Msh6p binds to and hydrolyses ATP.
MSH3	Mismatch repair protein; forms dimers with Msh2p that mediate repair of insertion or deletion mutations and removal of non-homologous DNA ends, contains a PCNA (Pol30p) binding motif required for genome stability.
MSH6	Protein required for mismatch repair in mitosis and meiosis; forms a complex with Msh2p to repair both single-base & insertion-deletion mispairs; also involved in interstrand cross-link repair.
PMS1	ATP-binding protein required for mismatch repair; required for both mitosis and meiosis; functions as a heterodimer with Mlh1p.
RAD1	Single-stranded DNA endonuclease (with Rad10p); cleaves single-stranded DNA during nucleotide excision repair and double-strand break repair.

RAD2	Single-stranded DNA endonuclease; cleaves single-stranded DNA during nucleotide excision repair to excise damaged DNA.
RLF2	Largest subunit (p90) of the Chromatin Assembly Complex (CAF-1); chromatin assembly by CAF-1 is important for multiple processes including silencing at telomeres, mating type loci, and rDNA; maintenance of kinetochore structure; deactivation of the DNA damage checkpoint after DNA repair; chromatin dynamics during transcription; and repression of divergent noncoding transcription.
SBA1	Co-chaperone that binds and regulates Hsp90 family chaperones; plays a role in determining prion variants; important for pp60v-src activity in yeast; homologous to the mammalian p23 proteins, and like p23 can regulate telomerase activity.
STM1	Protein required for optimal translation under nutrient stress; perturbs association of Yef3p with ribosomes; involved in TOR signalling; binds G4 quadruplex and purine motif triplex nucleic acid; helps maintain telomere structure.
SWD3	Essential subunit of the COMPASS (Set1C) complex; COMPASS methylates histone H3 on lysine 4 and is required in transcriptional silencing near telomeres.
TEL1	Protein kinase primarily involved in telomere length regulation; contributes to cell cycle checkpoint control in response to DNA damage; acts with Red1p and Mec1p to promote inter-homolog recombination by phosphorylation of Hop1; functionally redundant with Mec1p; regulates P-body formation induced by replication stress.
XRS2	Protein required for DNA repair; component of the Mre11 complex, which is involved in double strand breaks, meiotic recombination, telomere maintenance, and checkpoint signalling.
ZDS2	Protein with a role in regulating Swe1p-dependent polarized growth; involved in maintenance of Cdc55p in the cytoplasm where it promotes mitotic entry; interacts with silencing proteins at the telomere; implicated in the mitotic exit network through regulation of Cdc14p localization.